Tetratricopeptide repeat protein-associated proteins contribute to virulence of *Porphyromonas gingivalis.*

Yoshio Kondo[1,2], Naoya Ohara[3], Keiko Sato[1], Mamiko Yoshimura[4], Hideharu Yukitake[1], Mariko Naito[1], Taku Fujiwara[2], and Koji Nakayama[1,5,] *

[1]Division of Microbiology and Oral Infection, Department of Molecular Microbiology and Immunology, Nagasaki University Graduate School of Biomedical Sciences, Nagasaki 852-8588, Japan, [2]Department of Pediatric Dentistry, Nagasaki University Graduate School of Biomedical Sciences, Nagasaki 852-8588, Japan, [3]Department of Oral Microbiology, Okayama University Graduate School of Medicine , Dentistry and Pharmaceutical Sciences, Okayama 700-8558, Japan, [4]Department of Bacteriology, Osaka City University Graduate, School of Medicine, Osaka 545-8585, Japan, [5]Global COE Program at Nagasaki University, Nagasaki 852-8588, Japan

*Corresponding author: Koji Nakayama, D.D.S., Ph.D.

Division of Microbiology and Oral Infection, Department of Molecular Microbiology and Immunology, Nagasaki University Graduate School of Biomedical Sciences, 1-7-1 Sakamoto, Nagasaki 852-8588, Japan

Phone: 81-95-819-7648

Fax: 81-95-819-7650

E-mail: knak@nagasaki-u.ac.jp

ABSTRACT

Porphyromonas gingivalis is one of the most etiologically important microorganisms in periodontal disease. We found in a previous study that PG1385 (TprA) protein, a tetratricopeptide repeat (TPR) protein, was up-regulated in *P. gingivalis* wild-type cells placed in a mouse subcutaneous chamber and that a *tprA* mutant was clearly less virulent in the mouse subcutaneous abscess model. In this study, we investigated the gene expression profile of *tprA* mutant cells placed in a mouse subcutaneous chamber and found that 9 genes, including PG2102 (*tapA*), PG2101 (*tapB*) and PG2100 (*tapC*) genes, were down-regulated in the *tprA* mutant compared with those in the wild type. Expression of a cluster of *tapA*, *tapB* and *tapC* genes of the mutant was also down-regulated in an *in vitro* culture with enriched brain heart infusion. TprA protein has three TPR motifs, which are known as a protein-protein interaction module. Yeast two-hybrid system analysis and *in vitro* protein binding assays with immunoprecipitation and surface plasmon resonance detection revealed that TprA protein could bind to TapA and TapB proteins. TprA and TapB proteins were located in the periplasmic space, whereas TapA, which appeared to be one of the C-terminal domain family proteins, was located at the outer membrane. We constructed *tapA*, *tapB* and *tapC* single mutants and a *tapA-tapB-tapC* deletion mutant. In the mouse subcutaneous infection experiment, all of the mutants were less virulent than the wild type. These results suggest that TprA, TapA, TapB and TapC are cooperatively involved in *P. gingivalis* virulence.

INTRODUCTION

Periodontal disease, the major cause of tooth loss in the general population of industrial nations (21, 37), is a chronic inflammatory disease of the periodontium that leads to erosion of the attachment apparatus and supporting bone for the teeth (1) and is one of the most common infectious diseases of humans (36). The obligately anaerobic Gram-negative bacterium *Porphyromonas gingivalis* has become recognized as a major pathogen for chronic periodontitis (7). *P. gingivalis* has been found to express numerous potential virulence factors, such as fimbriae, hemagglutinins, lipopolysaccharides, and various proteases that are capable of hydrolyzing collagen, immunoglobulins, iron-binding proteins, and complement factors (16, 17). Expression of these virulence factors is thought to be tightly regulated in response to environmental cues. In recent years, the search for virulence factors has been greatly facilitated by molecular genetics (27). Although a number of studies have shown gene expression of *P. gingivalis* being regulated by environmental stresses (13, 19, 35, 38, 41, 46, 55), gene expression of *P. gingivalis* cells in *in vivo* lesions is not completely understood. Our previous study (54) using a subcutaneous chamber model showed that ten *P. gingivalis* proteins were up-regulated in host tissues, while four proteins were down-regulated. Among the up-regulated proteins, PG1089 (DNA-binding response regulator RprY), PG1385 (TPR domain protein) and PG2102 (immunoreactive 61 kDa antigen PG91) were chosen for further analysis. Mouse abscess model experiments revealed that a mutant strain defective in PG1385 was clearly less virulent and a mutant defective in PG2102 also had a tendency to be less virulent than the wild-type parent strain. These

results suggest that PG1385 and PG2102 proteins are involved in virulence of *P. gingivalis*.

PG1385 protein has three tetratricopeptide repeat (TPR) motifs. The TPR motif is a protein-protein interaction module found in multiple copies in a number of functionally different proteins that facilitate specific interactions with a partner protein(s) (3, 10).

In this study, we found that PG1385 protein bound to each of PG2101 and PG2102 proteins and that these mutant strains were less virulent, suggesting that PG1385, PG2101 and PG2102 proteins are cooperatively involved in *P. gingivalis* virulence.

MATERIALS AND METHODS

Strains and culture conditions. All *P. gingivalis* strains and plasmids used are shown in Table 1. *P. gingivalis* cells were grown anaerobically (10% CO_2, 10% H_2, 80% N_2) in enriched brain heart infusion (BHI) medium and on enriched tryptic soy (TS) agar. For selection and maintenance of the antibiotic-resistant strains, the antibiotics erythromycin (Em) and tetracycline (Tc) were added to the medium at concentrations of 10 μg/ml and 0.5 μg/ml, respectively.

Subcutaneous chamber model experiment. A subcutaneous chamber model experiment was performed according to Yoshimura *et al.* (54). Bacterial cells were grown at 37°C until an optical density at 550 nm (OD550) of 1.0 was reached.

Cultures were then concentrated by centrifugation at 10,000 x *g* for 10 min and cells were collected and resuspended in 1/30 of the original volume in fresh enriched BHI broth. Female BALB/c mice of 8 to 10 weeks in age were used. Coil-shaped subcutaneous chambers were prepared and surgically implanted as previously described by Genco *et al*. (15). One week after implantation, the chambers were inoculated with 0.4 ml of a concentrated suspension of *P. gingivalis* in enriched BHI broth. Ninety min after inoculation, chamber fluid containing bacterial cells was aseptically removed from each implanted chamber using a hypodermic needle (25-gauge) and syringe. Chamber fluid harvested from three mice was mixed and subjected to isolation of RNA for microarray analysis and real-time qPCR.

Microarray and data analyses. Bacterial cells were lysed in TRIzol Reagent (Invitrogen). RNA was isolated by TRIzol extraction followed by RNeasy column purification with genomic DNA digestion (DNase I) (Qiagen). Subsequently, synthesis of cDNA, target hybridization, washing and scanning were carried out according to the Affymetrix protocol. Gene chips for *P. gingivalis* W83 (TI242619 60mer), in which numbers of probes per target gene, replicates and total probes per chip were 19, 5 and 192,000, respectively, were purchased from Roche NimbleGen Inc. The gene chips were scanned, and the resulting image files were used to calculate and normalize the hybridization intensity data utilizing the GeneChip Operating Software (Affymetrix). Single microarray analysis measures a relative level of expression of a transcript (signal) and determines whether a transcript is present (P) or absent (A).

Absolute analysis of each microarray was followed by comparison analysis using GeneSpringGX7 software (Silicon Genetics). The comparison estimates the magnitude of change (i.e., the fold change of the normalized data) and the direction of the change (increase, decrease, or no change) of a transcript across the two arrays. Each experiment was performed twice, and only transcripts showing P/P were included here. Mean data for two sets of replicate samples were used for the comparison analysis. For most data sets, the results are shown as average fold change from the comparisons. A given transcript was designated as "up-regulated" when the average fold change increased at least 1.5 fold in expression level between two sets of replicate samples. A given transcript was designated as "down-regulated" when the average fold change decreased at least 1.5 fold in expression level between two sets of replicate samples.

Real-time qPCR. Total RNA was reverse-transcribed into cDNA with SuperScript III First Strand Synthesis System (Invitrogen). cDNA was used in real-time qPCR experiments performed in triplicate by using Brilliant® II Fast SYBR® Green QPCR Master Mix (Stratagene) with an Mx3005PTM Real-Time PCR System (Stratagene) according to the manufacturer's instructions. The primers for the real-time analysis (Table S1 in the supplemental material) were designed using Primer3 software (http://primer3.sourceforge.net/). Real-time qPCR conditions were as follows: 1 cycle at 95°C for 2 min and 35 cycles of 95°C for 5 sec and 60°C for 20 sec. At each cycle, accumulation of PCR products was detected by the reporter dye from the

dsDNA-binding SYBR Green. To confirm that a single PCR product was amplified, after the PCR, a dissociation curve (melting curve) was constructed in the range of 55°C to 95°C. All data were analyzed using Mx3005P software. The expression level of each targeted gene was normalized to that of *gyrA* (PG1386 encoding DNA gyrase A subunit) (31). All PCR reactions were carried out in triplicate. The efficiency of primer binding was determined by linear regression by plotting the cycle threshold (CT) value versus the log of the cDNA dilution. Relative quantification of the transcript was determined using the comparative CT method ($2^{-\Delta\Delta CT}$) calibrated to *gyrA*. qPCR experiments were performed three times independently with comparable results.

Subcellular fractionation. Subcellular fractionation of *P. gingivalis* cells was performed essentially according to Murakami *et al*. (26). *P. gingivalis* cells were harvested by centrifugation at 10,000 x *g* for 30 min at 4°C and resuspended with 20 ml of PBS containing 0.1 mM *N*-*p*-tosyl-L-lysine chloromethyl ketone (TLCK), 0.1 mM leupeptin, and 0.5 mM EDTA. The cells were disrupted in a French pressure cell at 100 MPa by two passes. The remaining intact bacterial cells were removed by centrifugation at 3,000 *g* for 10 min, and the supernatant was subjected to ultracentrifugation at 100,000 x *g* for 60 min. The cells were pelleted, and the supernatant was retained as the periplasmic/cytoplasmic fraction. The pellets were treated with 1% Triton X-100 in PBS containing 20 mM $MgCl_2$ for 30 min at 20°C. The outer membrane fraction was recovered as a precipitate by ultracentrifugation at 100,000 x *g* for 60 min at 4°C. The supernatant was obtained as the inner membrane

fraction.

Spheroplast formation and proteinase treatment. Spheroplast formation and proteinase treatment of *P. gingivalis* cells was essentially performed by the method described previously (12). After being suspended in 50 mM Tris acetate buffer (pH 7.8) containing 0.75 M sucrose, *P. gingivalis* cells were treated with lysozyme (final concentration, 0.1 mg/ml) on ice for 2 min. Conversion to spheroplasts was performed by slowly diluting the cell suspension over a period of 10 min with 2 volumes of cold 1.5 mM EDTA. After centrifugation at 10,000 x g for 10 min, the resulting precipitates were gently resuspended in 50 mM Tris acetate buffer (pH 7.8) containing 0.25 M sucrose and 10 mM $MgSO_4$ (spheroplasts). The supernatants were used as the periplasm fraction and the proteins in this fraction were precipitated with trichloroacetic acid and then subjected to SDS-PAGE and immunoblot analysis. Spheroplasts were treated on ice with proteinase K (final concentration, 1 mg/ml) in the presence or absence of 2% Triton X-100 for 1 h. After quenching proteinase K with phenylmethylsulfonyl fluoride (final concentration, 5 mM) for 5 min, the whole volume of the sample was mixed with 4 volumes of Laemmli sample buffer and subjected to SDS-PAGE and immunoblot analysis.

Protein electrophoresis and immunoblot analysis. SDS-PAGE was performed by using the method of Laemmli (23). The gels were stained with 0.1% Coomassie brilliant blue (CBB) R-250. For immunoblot analysis, proteins on SDS-PAGE gels were

electroblotted onto a PVDF membrane. The blots were blocked with 5% skim milk for 1 h at room temperature, probed with anti-PG1385, anti-PG2101, anti-PG2102, or MAb 1B5 overnight at 4°C, washed, incubated with HRP-conjugated secondary antibodies, and finally detected with ECL (GE Healthcare).

Protein purification and preparation of antisera. *P. gingivalis* W83 genome sequence data were obtained from the TIGR website (http://www.tigr.org). A genomic region including the PG1385 gene was amplified by PCR from the chromosomal DNA of *P. gingivalis* W83 with the primer pair 5-rPG1385/BamHI and 3-rPG1385/EcoRI using a PCR kit (Advantage-HF 2 PCR Kit; Clontech). The amplified DNA fragment was cloned into a T-vector (pGEM-T Easy; Promega) and digested with *Bam*HI and *Eco*RI. The resulting fragment was then inserted into the *Bam*HI-*Eco*RI region of pGEX-6P-1 (GE Healthcare), and the recombinant expression plasmid was then transformed into *E. coli* BL21 (DE3). *E. coli* BL21 (DE3) harboring the recombinant plasmid was inoculated into LB broth for large-scale culture. Isopropyl-β-D-thiogalactoside (IPTG) was added to the culture at a concentration of 0.1 mM, and this was followed by incubation for 3 h to overproduce the recombinant protein. The recombinant protein was purified with Glutathione Sepharose beads (GE Healthcare). For removal of the GST tag, the purified recombinant protein was incubated with PreScission proteases (GE Healthcare) at 4°C for 24 h. Then the protein was further purified and concentrated by using Amicon Ultra (Millipore).

Genomic regions including the PG2101 and PG2102 genes were amplified by PCR from the chromosomal DNA of *P. gingivalis* W83 with the primer pair 5-rPG2101/KpnI and 3-rPG2101/NotI for the PG2101 gene and with the primer pair 5-rPG2102/KpnI and 3-rPG2102/NotI for the PG2102 gene using the PCR kit. The

amplified DNA fragments were cloned into the T-vector and digested with *Kpn*I and *Not*I. The resulting fragments were then inserted into the *Kpn*I-*Not*I region of pET32a (Novagen) and the recombinant expression plasmids were then transformed into *Escherichia coli* BL21 (DE3). *E. coli* BL21 (DE3) harboring the recombinant plasmids was inoculated into LB broth for large-scale culture. IPTG was added to the culture at a concentration of 0.1 mM, and this was followed by incubation for 3 h to overproduce the recombinant proteins. The recombinant proteins were purified with a TALON Purification Kit (TAKARA Bio). Then the proteins were further purified and concentrated by using Amicon Ultra (Millipore).

Recombinant PG2101-His (rPG2101-His) protein was mixed with TiterMax Gold (TiterMax), and the mixtures were injected into mice (BALB/c) subcutaneously, resulting in anti-2101 antiserum. Anti-PG2101 IgG was purified from the antiserum obtained from mice using nProtein A sepharose (GE Healthcare). Polyclonal rabbit antisera against recombinant PG1385 (rPG1385) and PG2102-His (rPG2102-His) proteins were ordered from Sigma Genosys. Monoclonal antibody (MAb) 1B5 (9) was kindly provided by Michael A. Curtis.

Yeast two-hybrid system. The yeast two-hybrid system-3 was purchased from Clontech. An *Sau*3AI-digested genomic DNA of *P. gingivalis* W83 was inserted into the *Bam*HI site of pGADT7 to yield a genomic plasmid library. A genomic region including the PG1385 gene was amplified by PCR from the chromosomal DNA of *P. gingivalis* W83 with the primer pair Y2H-PG1385-Fw and Y2H-PG1385-Rv using

the PCR kit. The amplified DNA fragment was cloned into the T-vector and digested by *Nco*I and *Bam*HI. The resulting fragment was then inserted into the *Nco*I-*Bam*HI region of pGBKT7 to yield pKD1019. Competent yeast cells (strain AH109) containing pKD1019 were transformed with 15 μg of genomic plasmid library and were plated onto minimal synthetic dropout (SD) agar lacking tryptophan, leucine, and histidine. The plates were incubated at 30°C for 7 days, and then transformants were streaked onto fresh SD agar and tested further for their ability to hydrolyze X-β-Gal (5-bromo-4-chloro-3-indolyl--D-galactopyranoside).

Binding assays between rPG1385 and rPG2101-His and between rPG1385 and rPG2102-His. rPG1385 (0 to 1.0 μg) was dissolved in PBS and added to 500 ng of rPG2101-His or rPG2102-His in a final volume of 200 μl and then incubated at 4°C for 2 h. Following incubation, Ni^{2+}-chelate resin (Clontech) was added to the reaction mixture and incubated at 4°C for 2 h. Resin beads were recovered by centrifugation and washed 3 times with 500 μl of PBS. The opposite way for the above reaction was also analyzed. rPG1385 (500 ng) was dissolved in PBS and added to 0 to 1.0 μg of rPG2101-His or rPG2102-His in a final volume of 200 μl and then incubated at 4°C for 2 h. The resulting complexes were immunoprecipitated using anti-PG1385 antibody coupled with nProtein A sepharose (GE Healthcare) at 4 °C for 2 h. These precipitates were suspended in SDS-PAGE sample buffer and denatured by heating. Proteins on SDS-PAGE gels were blotted onto PVDF membranes and then subjected to immunoblotting using anti-PG1385, anti-PG2101 or anti-PG2102 antibody.

Surface plasmon resonance (BIACORE). The interaction of rPG1385 with rPG2101-His or rPG2102-His was determined with surface plasmon resonance detection (BIACORE X100, GE Healthcare). rPG1385 (20 μg/ml) in 10 mM sodium acetate (pH 5.5) was immobilized on a CM5 carboxymethyl-dextran sensor chip using the aminecoupling method. rPG2101-His or rPG2102-His (0.016 μM to 10 μM) in HBS-EP buffer (10 mM HEPES (pH 7.4) containing 150 mM NaCl, 3 mM EDTA and 0.005 % v/v Surfactant P 20) was passed over the surface of the sensor chip at a flow rate of 30 μl/ min. The interaction was monitored by determining changes in surface plasmon resonance response at 25°C. After 2 min of monitoring, the same buffer was introduced onto the sensor chip in place of the rPG1385 solution to start the dissociation. Both the association rate constant (*Ka*) and the dissociation rate constant (*Kd*) were calculated by using BIAevaluation software (GE Healthcare) and the program 1:1 (Langmuir) binding model. The dissociation constant (*KD*) was determined from *Kd*/*Ka*.

Construction of mutant strains. *P. gingivalis* PG2100 gene deletion mutant was constructed as follows. PG2100-upstream and PG2100-downstream DNA regions were PCR-amplified from *P. gingivalis* W83 chromosomal DNA using the primer pair 5-PG2100up/NotI and 3-PG2100up/BamHI for the PG2100-upstream region and the primer pair 5-PG2100dn/BamHI and 3-PG2100dn/KpnI for the PG2100-downstream region. The primers for the construction of mutant strains are listed in Table S1 in the

supplemental material. The amplified DNAs were cloned into the T-vector and digested with *Not*I and *Bam*HI for the PG2100-upstream DNA and with *Bam*HI and *Kpn*I for the PG2100-downstream DNA. The resulting fragments were inserted into the *Not*I-*Kpn*I region of pBluescript II SK(-) to yield pKD1008. The 1.5-kb *Bam*HI *ermF* DNA cartridge was inserted into the *Bam*HI site of pKD1008, resulting in pKD1009 (*⊿*PG2100::*ermF*). *P. gingivalis* W83 was then transformed with the *Bss*HII-linearized pKD1009 DNA to yield strain KDP386.

P. gingivalis PG2101, PG2102, and PG2102-PG2100 gene deletion mutants were constructed essentially the same as the PG2100 gene deletion mutant. The primer pair 5-PG2101up/NotI and 3-PG2101up/BamHI and the primer pair 5-PG2101dn/BamHI and 3-PG2101dn/KpnI were used for the PG2101-upstream region and the PG2101-downstream region in construction of the PG2101 gene deletion mutant, respectively. The primer pair 5-PG2102up/NotI and 3-PG2102up/BamHI and the primer pair 5-PG2102dn/BamHI and 3-PG2102dn/KpnI were used for the PG2102-upstream region and the PG2102-downstream region in construction of the PG2102 gene deletion mutant, respectively. The primer pair 5-PG2102up/NotI and 3-PG2102up/BamHI and the primer pair 5-PG2100dn/BamHI and 3-PG2100dn/KpnI were used for the PG2102-upstream region and the PG2100-downstream region in construction of the PG2102-PG2100 gene deletion mutant, respectively.

P. gingivalis porT deletion mutant was constructed as follows. *P. gingivalis* W83 was transformed with the *Bss*HII-linearized pKD357 (43) DNA to yield strain KDP385.

Immunoprecipitation. *P. gingivalis* cells were harvested and then dissolved with RIPA buffer (150 mM NaCl, 1% Nonidet P-40, 0.5% deoxycholate, 0.1% SDS and 50 mM Tris-HCl, pH 8.0) and immunoprecipitated by nProtein G agarose beads with 5 μg of anti-PG2102 polyclonal antibody. The resulting precipitate was dissolved with the same volume of the sample buffer and loaded on an SDS-10% gel. Immunoblot analysis was performed with the anti-*P. gingivalis* anionic surface polysaccarides monoclonal antibody MAb 1B5 (9).

Mouse virulence assay and statistical analysis. Virulence of *P. gingivalis* W83 and mutant strains was determined by mouse subcutaneous infection experiments (28, 49, 53). Bacterial cells were grown at 37°C until an OD550 of 1.0 was reached. The cells were harvested and then resuspended and adjusted to a concentration of approximately 1 x 10^{12} CFU/ml in the enriched BHI broth. Female BALB/c mice (8 to 10 weeks of age) were challenged with subcutaneous injections of 0.1 ml of bacterial suspension at two sites on the depilated dorsal surface (0.2 ml per mouse). Injected mice were examined daily for survival. Three sets of experiments were carried out.

For data analysis, Kaplan-Meier plots were made and the log-rank test was used to evaluate the difference in mean survival rates in three experiments between mice infected with W83 parent strain and those infected with the mutant strains.

RESULTS

Gene expression profiling of the PG1385 mutant (*tprA*) inoculated into a mouse subcutaneous chamber.

We previously found that a strain defective in the PG1385 gene was clearly less virulent than the wild-type strain, indicating that PG1385 protein was involved in *P. gingivalis* virulence (54). The PG1385 gene encodes a TPR protein and is designated *tprA*. To investigate whether loss of the *tprA* gene product (TprA) influences *in vivo* expression of *P. gingivalis* genes, we determined the *in vivo* gene expression profile of the *tprA* mutant that was inoculated in a mouse subcutaneous chamber by using microarray analysis. Coil-shaped subcutaneous chambers were surgically implanted as previously described by Genco *et al*. (15). One week after implantation, *P. gingivalis* cells were inoculated into mouse subcutaneous chambers. Chamber fluid containing bacterial cells was aseptically removed from each implanted chamber 90 min after inoculation and subjected to isolation of total RNA for microarray analysis.

Genes of the *tprA* mutant with an average expression more than 1.5-fold (up or down) relative to those of the wild-type parent were identified since the threshold was reported to be biologically significant (20, 24, 48). In the *tprA* mutant, 11 genes were up-regulated, while 12 genes were down-regulated (Table 2). We found that the up-regulated genes were related to protein synthesis and hypothetical protein, grouped by TIGR functional role categories. Interestingly, PG1055 (thiol protease) and PG2102 (immunoreactive 61-kDa antigen PG91), which were up-regulated in *P. gingivalis* wild-type cells placed in a mouse subcutaneous chamber (54), were found to be down-regulated in the *tprA* mutant. To confirm the results obtained by microarray

analysis, the RNA samples were subjected to real-time qPCR analysis. The expression of *gyrA* (gene encoding a putative DNA gyrase A subunit, PG1386) was used for normalization. The 12 down-regulated genes in microarray analysis were examined using real-time qPCR, showing that 9 of the 12 genes were down-regulated (Fig. 1). Genes for PG0162 (RNA polymerase sigma-70 factor, ECF subfamily), PG1055, PG2100 (immunoreactive 63-kDa antigen PG102), PG2101 (hypothetical protein) and PG2102 were markedly down-regulated. Down-regulation of genes for PG2100, PG2101 and PG2102 in the *tprA* mutant was also observed in cells incubated in enriched BHI medium (Fig. S1 in the supplemental material).

To determine whether PG2102-, PG2101- and PG2100-encoding genes, which are designated *tapA* (TprA-associated protein A gene), *tapB* and *tapC*, respectively, are polycistronically transcribed, total RNA of the wild-type strain was subjected to PCR analysis. Total RNA was isolated from the wild-type strain, then cDNA was synthesized, and gene-specific primers were used for amplifying junction DNA among these genes. The junction DNA between the *tapA* and *tapB* genes and between the *tapB* and *tapC* genes was amplified, suggesting that these genes make up of an operon (Fig. S2 in the supplemental material).

Yeast two-hybrid analysis

As another approach to clarify the molecular mechanism of contribution of TprA protein to *P. gingivalis* virulence, we attempted to find *P. gingivalis* proteins that interacted with TprA protein since it is likely that TprA protein, which is one of the TPR

domain-containing proteins (3, 10), is associated with other proteins. Firstly, we investigated the localization of TprA protein. The *tprA* mutant and its wild-type parent were fractionated into cytoplasm/periplasm, inner membrane and outer membrane fractions and then subjected to SDS-PAGE and immunoblot analysis with anti-TprA antiserum (Fig. 2A). An anti-TprA-immunoreactive protein was found at a molecular mass of 43 kDa in the cytoplasm/periplasm fraction. For further analysis, spheroplast formation and proteinase K treatment was performed (Fig. 2B). The 43-kDa anti-TprA immunoreactive protein band was observed in the periplasmic fraction. The 43-kDa protein, which was degraded by treatment with proteinase K, was also detected in the spheroplast fraction. In addition, TprA protein possessed a signal sequence as revealed by *in silico* analysis with the software SignalP V3.0 (http://www.cbs.dtu.dk/services/SignalP/) (2). These results clearly indicate that TprA protein is located in the periplasmic space, which is consistent with results of a previous study (45).

Yeast two-hybrid analysis was then performed using the *tprA* gene as bait. A number of *P. gingivalis* protein candidates interacting with TprA protein were found in the analysis (Table 3). They included PG0415 (peptidyl-prolyl cis-trans isomerase, PPIC-type), PG0497 (5'-methylthioadenosine/S-adenosylhomocysteine nucleosidase), PG1334 (band 7/Mec-2 family protein), PG2101 (TapB) and PG2200 (TPR domain protein) as a putative periplasmic protein.

Specific binding of TprA protein with TapA and TapB proteins

We examined the interaction of TprA protein with TapA, TapB and TapC proteins *in vitro* using protein binding assays. We determined the binding activity of TprA protein with TapA and TapB proteins since we could not obtain a TapC soluble recombinant protein (Fig. 3). Poly-histidine-tagged recombinant TapA (rTapA-His) or TapB (rTapB-His) was incubated with Ni-beads and recombinant TprA (rTprA). rTprA itself did not bind to Ni-beads, as revealed by immunoblot analysis using anti-TprA antibody, while rTprA could bind to Ni-beads in the presence of rTapA-His or rTapB-His, and the reaction was observed in a concentration-dependent manner (Fig. 3A, C). Next, rTprA was mixed with rTapA-His or rTapB-His, immunoprecipitated with anti-TprA antibody, and subjected to immunoblot analysis with anti-TapA or anti-TapB antibody. The results were consistent with the above results (Fig. 3B, D).

These specific interactions were further confirmed by surface plasmon resonance detection using the BIAcore system. The K_d values of interactions of rTprA with rTapA-His and rTapB-His were 1.89×10^{-4} M and 1.42×10^{-6} M, respectively (Fig. 4).

Localization of TapA and TapB proteins

Cells of the wild-type and *tapB* mutant strains were fractionated into cytoplasm/periplasm, inner membrane and outer membrane fractions and then subjected to SDS-PAGE and immunoblot analysis with anti-TapB antiserum (Fig. 5A). A 33-kDa anti-TapB-immunoreactive protein was found in the cytoplasm/periplasm fraction. To determine whether the 33-kDa anti-TapB-immunoreactive protein was located in the cytoplasm or periplasm, cells of the wild-type strain were subjected to

spheroplast formation and proteinase K treatment followed by immunoblot analysis with anti-TapB (Fig. 5B). The 33-kDa anti-TapB-immunoreactive protein was found in the periplasm fraction. The 33-kDa protein was also found in the spheroplast fraction and disappeared after the proteinase K treatment. TapB protein possessed a signal sequence as revealed by *in silico* analysis with the software SignalP V3.0. These results indicated periplasmic localization of TapB.

To investigate the localization of TapA protein, the wild-type and *tapA* mutant cells were fractionated into cytoplasm/periplasm, inner membrane and outer membrane fractions and then subjected to SDS-PAGE and immunoblot analysis with anti-TapA (Fig. 5C). A discrete protein band with a molecular mass of 60 kDa and diffuse protein bands with molecular masses of 65-95 kDa were detected in the outer membrane fraction of the wild-type strain but not in that of the *tapA* mutant. These protein bands were also observed in the cytoplasmi/periplasm fraction with much weaker reaction. These results indicated that TapA protein was located at the outer membrane.

TapA is one of the CTD proteins.

P. gingivalis has been shown to possess a novel family of outer membrane proteins that have a conserved C-Terminal Domain (CTD) of RgpB (45, 51). The CTD has been proposed to play roles in the secretion of the proteins across the outer membrane and their attachment to the cell surface, probably via glycosylation (30, 43, 45). Very recently, we have found a novel secretion system, Por secretion system (PorSS), by which the CTD proteins may be secreted (42).

TapA (PG2102) was reported to belong to the CTD family of proteins and seemed to be secreted across the outer membrane and attach to the cell surface via glycosylation. TapA protein was immunoprecipitated from the wild-type, *porT* and *tapA* mutant strains using anti-TapA. The immunoprecipitates were subjected to SDS-PAGE and immunoblot analysis using a monoclonal antibody, MAb 1B5, which recognizes *P. gingivalis* anionic surface polysaccharides. MAb 1B5-immunoreactive diffuse protein bands with molecular masses of 65-95 kDa were found in the wild-type strain but not in the *porT* or *tapA* mutant strain (Fig. 6). The results suggested that the MAb 1B5-immunoreactive diffuse protein bands with molecular masses of 65-95 kDa were glycosylated forms of TapA protein. In the *porT* mutant, the anti-TapA-immunoreactive protein with a molecular mass of 60 kDa was mainly found in the cytoplasm/periplasm fraction, suggesting that TapA protein is one of the outer membrane proteins secreted via PorSS.

Contribution of the *tapA-tapB-tapC* operon to virulence of *P. gingivalis*

BALB/c mice were challenged with subcutaneous injections of bacterial suspension (2 x 10^{11} colony-forming units (CFU) per animal) (28, 49, 53), and their survival was monitored for 9 days. About 66.7% of the mice challenged with W83 died at the end of the experiment (9 days). In contrast, the survival rates of mice inoculated with the *tprA*, *tapA*, *tapB* and *tapC* single mutants and the *tapA-tapB-tapC* deletion mutant were significantly higher ($P < 0.05$, log-rank test) than that of mice inoculated with the wild-type strain (Fig. 7). These results suggested that the *tprA, tapA, tapB* and *tapC*

genes were involved in *P. gingivalis* virulence.

DISCUSSION

The TPR motif was originally reported for cell division cycle proteins of *Saccharomyces cerevisiae* (18, 47). This motif is now known to be ubiquitous in nature, as it is found within functionally unrelated proteins from all genera. A TPR is defined as a degenerate 34-residue motif with a consensus amino acid arrangement of alternate large and small residues and high amino acid conservation observed specifically at positions 8, 20, and 27 (47). These conserved residues allow the TPR to create a pair of antiparallel alpha helices. Multiple motifs, ranging from 3 to 16 in number among TPR proteins, lead to the formation of an alpha superhelical structure (11). This complex and unique structure gives rise to distinct substrate grooves that facilitate specific protein-protein interactions. The ability of TPR-containing proteins to interact with other proteins enables them to play a vital role in eukaryotic cell processes, such as mitosis, transcription repression, and protein import (14, 22, 50). Bacteria also utilize TPR proteins for a range of functions, including gene regulation, flagellar motor function, chaperone activity, gliding motility and virulence (4, 5, 8, 29, 34, 44, 52). For example, FrzF from *Myxococcus xanthus* is a methyltransferase containing three TPR domains and it regulates the Frz chemosensory system, which controls cell reversals and gliding motility. In particular, TPRs in FrzF are involved in site-specific methylation of FrzCD, a metlyl-accepting chemotaxis protein (44). In addition, several chaperones required for the type III secretion system contain a TPR domain, including PcrH from

Pseudomonas aeruginosa, LcrH from *Yersinia* species, and CesD from enteropathogenic *Escherichia coli* (4, 5, 52).

P. gingivalis W83 has at least ten TPR proteins. However, none of them have been investigated so far. Structures of the TPR proteins are depicted with their putative subcellular location in Fig. S4 in the supplemental material. TprA protein contains three TPR domains. Okano *et al*. (35) reported that 19 proteins of *P. gingivalis* W83 are up-regulated by aeration and that the 19 proteins include PG1385 (TprA), PG0045 (HtpG), PG0520 (60-kDa chaperonin), PG1208 (DnaK), PG0762 (trigger factor), PG0185 (RagA) and PG0618 (AhpC). Masuda *et al*. (25) reported that 14 proteins including TprA are up-regulated in *P. gingivalis* ATCC 33277 cells cultivated in a nutrient-poor medium. We have reported that TprA protein was up-regulated in *P. gingivalis* W83 cells placed in a mouse subcutaneous chamber (54). Mouse subcutaneous infection experiments revealed that the *tprA* mutant was clearly less virulent. These findings suggest that expression of *tprA* is influenced by various environmental stresses and that TprA is involved in virulence of *P. gingivalis*.

TprA protein is located at the periplasm (45), implying that TprA binds to other proteins at the periplasm or protruding from the inner or outer membrane. We performed a yeast two-hybrid assay and found TapB (hypothetical protein) as a TprA-associated protein. Taken together with the finding that expression of TapA was induced in *P. gingivalis* cells placed in a mouse chamber as well as TprA, we assumed that TprA was related with products of a cluster of *tapA*, *tapB* and *tapC* genes. Protein binding assays with immunoprecipitation and plasmon resonance detection revealed the

interaction of TprA protein with TapA and TapB proteins. We could not examine the interaction between TprA protein and TapC protein in this study; however, TapC protein may interact with TprA protein since TapC protein has 45% identity in amino acid sequence with TapA protein. Mouse subcutaneous infection experiments in this study revealed that the survival rate of mice with the *tprA* mutant was equivalent to that of mice with the *tapA-tapB-tapC* deletion mutant, suggesting that TprA protein plays a role in virulence of *P. gingivalis* in cooperation with TapA, TapB and TapC proteins.

We also investigated the gene expression profile of the *tprA* mutant inoculated into a mouse subcutaneous chamber compared with the wild-type strain by using a microarray. The results of microarray analysis revealed that 12 genes were up-regulated and 11 genes were down-regulated in the *tprA* mutant. Interestingly, a cluster of *tapA*, *tapB* and *tapC* genes was found to be down-regulated in the *tprA* mutant strain. Down-regulation of the *tapA*, *tapB* and *tapC* genes was confirmed by real-time qPCR analysis. At present, the mechanism of down-regulation remains to be clarified.

TapA and TapC proteins belong to the C-Terminal Domain (CTD) family of proteins (45). The CTD has been proposed to play roles in the secretion of proteins across the outer membrane and their attachment to the surface of the cell, probably via glycosylation (30, 43, 45). Nguyen *et al*. reported that CTD is specifically conserved in proteins of distinct members of the phylum *Bacteroidetes* and suggested that CTD proteins are secreted by a novel secretion system. Very recently, we have found a novel secretion system by which CTD proteins are secreted and named it Por secretion system (PorSS) (42). We found in the present study that TapA protein, which was an outer

membrane protein, was modified by polysaccharides immunoreactive to the MAb 1B5, resulting in production of diffuse protein bands with molecular masses of 65-95 kDa, which were lacking in the *porT* mutant. These results suggest that TapA protein is secreted by PorSS.

As revealed by the mouse subcutaneous infection experiments, the *tapA* and *tapC* mutants were less virulent than the wild-type parent strain, suggesting that the CTD proteins TapA and TapC were related to virulence of *P. gingivalis*. Besides TapA and TapC proteins, *P. gingivalis* has a number of CTD proteins: gingipain proteinases (RgpA, RgpB and Kgp), CPG70 carboxypeptidase (6), PrtT thiol proteinase, HagA haemagglutinin, *Streptococcus gordonii* binding protein (55), putative haemagglutinin, putative thiol reductase, putative fibronectin binding protein, putative Lys-specific proteinase and putative von Willebrand factor domain protein. RgpA and Kgp contain C-terminal adhesins that are secreted and processed to form non-covalent complexes on the cell surface and are considered to be the major virulence factors of this bacterium (32, 33, 40). Gingipains have been linked directly to disease pathogenesis due to their ability to degrade host structural and defense proteins and the inability of mutants lacking functional Kgp or RgpA/B to cause alveolar bone loss in murine periodontitis models (39). The majority of these proteins are likely to play important roles in virulence of the bacterium since they are involved in extracellular proteolytic activity, aggregation, heme/iron capture and storage, biofilm formation and resistance to oxidative stress.

ACKNOWLEDGMENTS

This work was supported by Grant-in-Aids (18018032 and 20249073 to K.N.) for Scientific Research from the Ministry of Education, Culture, Sports, Science and Technology of Japan and by the Global COE Program at Nagasaki University to K.N.

REFFERENCES

1. **Armitage, G. C.** 1996. Periodontal diseases: diagnosis. Ann Periodontol **1:**37-215.
2. **Bendtsen, J. D., H. Nielsen, G. von Heijne, and S. Brunak.** 2004. Improved prediction of signal peptides: SignalP 3.0. J Mol Biol **340:**783-795.
3. **Blatch, G. L., and M. Lassle.** 1999. The tetratricopeptide repeat: a structural motif mediating protein-protein interactions. Bioessays **21:**932-939.
4. **Broms, J. E., P. J. Edqvist, A. Forsberg, and M. S. Francis.** 2006. Tetratricopeptide repeats are essential for PcrH chaperone function in *Pseudomonas aeruginosa* type III secretion. FEMS Microbiol Lett **256:**57-66.
5. **Broms, J. E., A. L. Forslund, A. Forsberg, and M. S. Francis.** 2003. PcrH of *Pseudomonas aeruginosa* is essential for secretion and assembly of the type III translocon. J Infect Dis **188:**1909-1921.
6. **Chen, Y. Y., K. J. Cross, R. A. Paolini, J. E. Fielding, N. Slakeski, and E. C. Reynolds.** 2002. CPG70 is a novel basic metallocarboxypeptidase with C-terminal polycystic kidney disease domains from *Porphyromonas gingivalis*. J Biol Chem **277:**23433-23440.
7. **Christersson, L. A., C. L. Fransson, R. G. Dunford, and J. J. Zambon.** 1992. Subgingival distribution of periodontal pathogenic microorganisms in adult periodontitis. J Periodontol **63:**418-425.
8. **Core, L., and M. Perego.** 2003. TPR-mediated interaction of RapC with ComA inhibits response regulator-DNA binding for competence development in *Bacillus subtilis*. Mol Microbiol **49:**1509-1522.
9. **Curtis, M. A., A. Thickett, J. M. Slaney, M. Rangarajan, J. Aduse-Opoku, P. Shepherd, N. Paramonov, and E. F. Hounsell.** 1999. Variable carbohydrate modifications to the catalytic chains of the RgpA and RgpB proteases of *Porphyromonas gingivalis* W50. Infect Immun **67:**3816-3823.
10. **D'Andrea, L. D., and L. Regan.** 2003. TPR proteins: the versatile helix. Trends Biochem Sci **28:**655-662.
11. **Das, A. K., P. W. Cohen, and D. Barford.** 1998. The structure of the tetratricopeptide repeats of protein phosphatase 5: implications for

TPR-mediated protein-protein interactions. EMBO J **17:**1192-1199.

12. **Delgado-Partin, V. M., and R. E. Dalbey.** 1998. The proton motive force, acting on acidic residues, promotes translocation of amino-terminal domains of membrane proteins when the hydrophobicity of the translocation signal is low. J Biol Chem **273:**9927-9934.
13. **Diaz, P. I., N. Slakeski, E. C. Reynolds, R. Morona, A. H. Rogers, and P. E. Kolenbrander.** 2006. Role of oxyR in the oral anaerobe *Porphyromonas gingivalis*. J Bacteriol **188:**2454-2462.
14. **Dodt, G., and S. J. Gould.** 1996. Multiple PEX genes are required for proper subcellular distribution and stability of Pex5p, the PTS1 receptor: evidence that0 PTS1 protein import is mediated by a cycling receptor. J Cell Biol **135:**1763-1774.
15. **Genco, C. A., C. W. Cutler, D. Kapczynski, K. Maloney, and R. R. Arnold.** 1991. A novel mouse model to study the virulence of and host response to *Porphyromonas* (*Bacteroides*) *gingivalis*. Infect Immun **59:**1255-1263.
16. **Grenier, D., and D. Mayrand.** 1987. Selected characteristics of pathogenic and nonpathogenic strains of *Bacteroides gingivalis*. J Clin Microbiol **25:**738-740.
17. **Haffajee, A. D., and S. S. Socransky.** 1994. Microbial etiological agents of destructive periodontal diseases. Periodontol 2000 **5:**78-111.
18. **Hirano, T., N. Kinoshita, K. Morikawa, and M. Yanagida.** 1990. Snap helix with knob and hole: essential repeats in S. pombe nuclear protein nuc2+. Cell **60:**319-328.
19. **Hosogi, Y., and M. J. Duncan.** 2005. Gene expression in *Porphyromonas gingivalis* after contact with human epithelial cells. Infect Immun **73:**2327-2335.
20. **Hughes, T. R., M. J. Marton, A. R. Jones, C. J. Roberts, R. Stoughton, C. D. Armour, H. A. Bennett, E. Coffey, H. Dai, Y. D. He, M. J. Kidd, A. M. King, M. R. Meyer, D. Slade, P. Y. Lum, S. B. Stepaniants, D. D. Shoemaker, D. Gachotte, K. Chakraburtty, J. Simon, M. Bard, and S. H. Friend.** 2000. Functional discovery via a compendium of expression profiles. Cell **102:**109-126.
21. **Irfan, U. M., D. V. Dawson, and N. F. Bissada.** 2001. Epidemiology of periodontal disease: a review and clinical perspectives. J Int Acad Periodontol **3:**14-21.

22. **King, R. W., J. M. Peters, S. Tugendreich, M. Rolfe, P. Hieter, and M. W. Kirschner.** 1995. A 20S complex containing CDC27 and CDC16 catalyzes the mitosis-specific conjugation of ubiquitin to cyclin B. Cell **81:**279-288.

23. **Laemmli, U. K.** 1970. Cleavage of structural proteins during the assembly of the head of bacteriophage T4. Nature **227:**680-685.

24. **Lo, A. W., C. A. Seers, J. D. Boyce, S. G. Dashper, N. Slakeski, J. P. Lissel, and E. C. Reynolds.** 2009. Comparative transcriptomic analysis of *Porphyromonas gingivalis* biofilm and planktonic cells. BMC Microbiol **9:**18.

25. **Masuda, T., Y. Murakami, T. Noguchi, and F. Yoshimura.** 2006. Effects of various growth conditions in a chemostat on expression of virulence factors in *Porphyromonas gingivalis*. Appl Environ Microbiol **72:**3458-3467.

26. **Murakami, Y., M. Imai, H. Nakamura, and F. Yoshimura.** 2002. Separation of the outer membrane and identification of major outer membrane proteins from *Porphyromonas gingivalis*. Eur J Oral Sci **110:**157-162.

27. **Nakayama, K.** 2003. Molecular genetics of *Porphyromonas gingivalis*: gingipains and other virulence factors. Curr Protein Pept Sci **4:**389-395.

28. **Neiders, M. E., P. B. Chen, H. Suido, H. S. Reynolds, J. J. Zambon, M. Shlossman, and R. J. Genco.** 1989. Heterogeneity of virulence among strains of *Bacteroides gingivalis*. J Periodontal Res **24:**192-198.

29. **Newton, H. J., F. M. Sansom, J. Dao, A. D. McAlister, J. Sloan, N. P. Cianciotto, and E. L. Hartland.** 2007. Sel1 repeat protein LpnE is a *Legionella pneumophila* virulence determinant that influences vacuolar trafficking. Infect Immun **75:**5575-5585.

30. **Nguyen, K. A., J. Travis, and J. Potempa.** 2007. Does the importance of the C-terminal residues in the maturation of RgpB from *Porphyromonas gingivalis* reveal a novel mechanism for protein export in a subgroup of Gram-Negative bacteria? J Bacteriol **189:**833-843.

31. **Nguyen, K. A., J. Zylicz, P. Szczesny, A. Sroka, N. Hunter, and J. Potempa.** 2009. Verification of a topology model of PorT as an integral outer-membrane protein in *Porphyromonas gingivalis*. Microbiology **155:**328-337.

32. **NM, O. B.-S., P. D. Veith, S. G. Dashper, and E. C. Reynolds.** 2003. *Porphyromonas gingivalis* gingipains: the molecular teeth of a microbial vampire. Curr Protein Pept Sci **4:**409-426.

33. **O'Brien-Simpson, N. M., R. A. Paolini, B. Hoffmann, N. Slakeski, S. G. Dashper, and E. C. Reynolds.** 2001. Role of RgpA, RgpB, and Kgp proteinases in virulence of *Porphyromonas gingivalis* W50 in a murine lesion model. Infect Immun **69:**7527-7534.

34. **Okabe, M., T. Yakushi, and M. Homma.** 2005. Interactions of MotX with MotY and with the PomA/PomB sodium ion channel complex of the *Vibrio alginolyticus* polar flagellum. J Biol Chem **280:**25659-25664.

35. **Okano, S., Y. Shibata, T. Shiroza, and Y. Abiko.** 2006. Proteomics-based analysis of a counter-oxidative stress system in *Porphyromonas gingivalis*. Proteomics **6:**251-258.

36. **Oliver, R. C., L. J. Brown, and H. Loe.** 1998. Periodontal diseases in the United States population. J Periodontol **69:**269-278.

37. **Papapanou, P. N.** 1999. Epidemiology of periodontal diseases: an update. J Int Acad Periodontol **1:**110-116.

38. **Park, Y., O. Yilmaz, I. Y. Jung, and R. J. Lamont.** 2004. Identification of *Porphyromonas gingivalis* genes specifically expressed in human gingival epithelial cells by using differential display reverse transcription-PCR. Infect Immun **72:**3752-3758.

39. **Pathirana, R. D., N. M. O'Brien-Simpson, G. C. Brammar, N. Slakeski, and E. C. Reynolds.** 2007. Kgp and RgpB, but not RgpA, are important for *Porphyromonas gingivalis* virulence in the murine periodontitis model. Infect Immun **75:**1436-1442.

40. **Potempa, J., R. Pike, and J. Travis.** 1995. The multiple forms of trypsin-like activity present in various strains of *Porphyromonas gingivalis* are due to the presence of either Arg-gingipain or Lys-gingipain. Infect Immun **63:**1176-1182.

41. **Rodrigues, P. H., and A. Progulske-Fox.** 2005. Gene expression profile analysis of *Porphyromonas gingivalis* during invasion of human coronary artery endothelial cells. Infect Immun **73:**6169-6173.

42. **Sato, K., M. Naito, H. Yukitake, H. Hirakawa, M. Shoji, M. J. McBride, R. G. Rhodes, and K. Nakayama.** 2010. A protein secretion system linked to bacteroidete gliding motility and pathogenesis. Proc. Natl. Acad. Sci. U.S.A. **107**: 276-281.

43. **Sato, K., E. Sakai, P. D. Veith, M. Shoji, Y. Kikuchi, H. Yukitake, N. Ohara,**

M. Naito, K. Okamoto, E. C. Reynolds, and K. Nakayama. 2005. Identification of a new membrane-associated protein that influences transport/maturation of gingipains and adhesins of *Porphyromonas gingivalis*. J Biol Chem **280:**8668-8677.

44. **Scott, A. E., E. Simon, S. K. Park, P. Andrews, and D. R. Zusman.** 2008. Site-specific receptor methylation of FrzCD in *Myxococcus xanthus* is controlled by a tetra-trico peptide repeat (TPR) containing regulatory domain of the FrzF methyltransferase. Mol Microbiol **69:**724-735.
45. **Seers, C. A., N. Slakeski, P. D. Veith, T. Nikolof, Y. Y. Chen, S. G. Dashper, and E. C. Reynolds.** 2006. The RgpB C-terminal domain has a role in attachment of RgpB to the outer membrane and belongs to a novel C-terminal-domain family found in *Porphyromonas gingivalis*. J Bacteriol **188:**6376-6386.
46. **Shelburne, C. E., R. M. Gleason, G. R. Germaine, L. F. Wolff, B. H. Mullally, W. A. Coulter, and D. E. Lopatin.** 2002. Quantitative reverse transcription polymerase chain reaction analysis of *Porphyromonas gingivalis* gene expression in vivo. J Microbiol Methods **49:**147-156.
47. **Sikorski, R. S., M. S. Boguski, M. Goebl, and P. Hieter.** 1990. A repeating amino acid motif in CDC23 defines a family of proteins and a new relationship among genes required for mitosis and RNA synthesis. Cell **60:**307-317.
48. **Smoot, L. M., J. C. Smoot, M. R. Graham, G. A. Somerville, D. E. Sturdevant, C. A. Migliaccio, G. L. Sylva, and J. M. Musser.** 2001. Global differential gene expression in response to growth temperature alteration in group A Streptococcus. Proc Natl Acad Sci U S A **98:**10416-10421.
49. **Tachibana-Ono, M., A. Yoshida, S. Kataoka, T. Ansai, Y. Shintani, Y. Takahashi, K. Toyoshima, and T. Takehara.** 2008. Identification of the genes associated with a virulent strain of *Porphyromonas gingivalis* using the subtractive hybridization technique. Oral Microbiol Immunol **23:**84-87.
50. **Tzamarias, D., and K. Struhl.** 1994. Functional dissection of the yeast Cyc8-Tup1 transcriptional co-repressor complex. Nature **369:**758-761.
51. **Veith, P. D., G. H. Talbo, N. Slakeski, S. G. Dashper, C. Moore, R. A. Paolini, and E. C. Reynolds.** 2002. Major outer membrane proteins and proteolytic processing of RgpA and Kgp of *Porphyromonas gingivalis* W50. Biochem J

363:105-115.

52. **Wattiau, P., B. Bernier, P. Deslee, T. Michiels, and G. R. Cornelis.** 1994. Individual chaperones required for Yop secretion by Yersinia. Proc Natl Acad Sci U S A **91:**10493-10497.

53. **Yoshimura, M., Y. Nakano, Y. Yamashita, T. Oho, T. Saito, and T. Koga.** 2000. Formation of methyl mercaptan from L-methionine by *Porphyromonas gingivalis*. Infect Immun **68:**6912-6916.

54. **Yoshimura, M., N. Ohara, Y. Kondo, M. Shoji, S. Okano, Y. Nakano, Y. Abiko, and K. Nakayama.** 2008. Proteome analysis of *Porphyromonas gingivalis* cells placed in a subcutaneous chamber of mice. Oral Microbiol Immunol **23:**413-418.

55. **Zhang, Y., T. Wang, W. Chen, O. Yilmaz, Y. Park, I. Y. Jung, M. Hackett, and R. J. Lamont.** 2005. Differential protein expression by *Porphyromonas gingivalis* in response to secreted epithelial cell components. Proteomics **5:**198-211.

FIGURE LEGENDS

Fig. 1. Real-time qPCR analysis of gene expression in the *tprA* mutant inoculated into a mouse subcutaneous chamber.

Mouse subcutaneous chamber experiments were performed as described in "Materials and Methods." Total RNA was extracted from W83 (wild type) and KDP159 (*tprA*::*ermF*). The down-regulated genes revealed by microarray analysis were selected for analysis by real-time qPCR. All PCR reactions were carried out in triplicate.

Fig. 2. Subcellular localization of TprA protein.

(A) Cytoplasm/periplasm, total membrane, inner membrane and outer membrane

fractions. Cells of W83 (wild type) and KDP159 (*tprA*::*ermF*) were fractionated and subjected to SDS-PAGE and immunoblot analysis using anti-TprA antiserum. Lanes: 1, cytoplasm/periplasm fraction; 2, total membrane fraction; 3, inner membrane fraction; 4, outer membrane fraction. (B) Spheroplast and periplasm fractions. Preparation of spheroplasts of *P. gingivalis* cells was performed as described in "Materials and Methods" and the spheroplasts were subjected to proteinase K treatment (Pro K) in the presence or absence of 2% Triton X-100 (TX-100). Samples were subjected to SDS-PAGE followed by immunoblot analysis with anti-TprA antiserum. Sph, spheroplasts; Peri, periplasm fraction.

Fig. 3. Binding of TprA protein to TapA and TapB proteins.

(A, B) Binding of TprA and TapB. rTprA (0 to 1.0 μg) was mixed with rTapB-His (0.5 μg) and was affinity-purified by Ni-beads. The resulting samples were subjected to SDS-PAGE and immunoblot analysis with anti-TprA (A). rTapB-His (0 to 1.0 μg) was mixed with rTprA (0.5 μg) and was immuno-purified by protein G agarose with anti-TprA. The resulting samples were subjected to SDS-PAGE and immunoblot analysis with anti-TapB (B). (C, D) Binding of TprA and TapA. rTprA (0 to 1.0 μg) was mixed with rTapA-His (0.5 μg) and was affinity-purified by Ni-beads. The resulting samples were subjected to SDS-PAGE and immunoblot analysis with anti-TprA (C). rTapA-His (0 to 1.0 μg) was mixed with rTprA (0.5 μg) and was immuno-purified by protein G agarose with anti-TprA. The resulting samples were subjected to SDS-PAGE and immunoblot analysis with anti-TapA (D).

Fig. 4. Surface plasmon resonance detection.

Parameters of association and dissociation for rTapA-His and rTapB-His with rTprA were determined by surface plasmon resonance analysis (Biacore). Sensorgrams for the binding of rTapA-His or rTapB-His to rTprA immobilized on a CM5 sensor chip were overlaid at various concentrations of rTapA-His or rTapB-His. rTapA-His, rTapB-His or bovine serum albumin (BSA) was injected at the concentrations of 0.016, 0.08, 0.4, 2 and 10 mM. The K_d values of binding of rTprA to rTapA-His and rTapB-His were 1.89 x 10^{-4}M and 1.42 x 10^{-6} M, respectively.

Fig. 5. Localization of TapA and TapB proteins.

(A, B) Subcellular localization of TapB protein. Fractions of cytoplasm/periplasm (lane 1) and total membrane (lane 2) of W83 (wild type) and KDP382 (*ΔtapB*::*ermF*) were subjected to SDS-PAGE and immunoblot analysis using anti-TapB (A). Spheroplast and periplasm fractions of *P. gingivalis* cells were separated as described in "Materials and Methods." Spheroplasts were subjected to the proteinase K treatment (Pro K) in the presence or absence of 2% Triton X-100 (TX-100). Samples were subjected to SDS-PAGE followed by immunoblot analysis with anti-TapB (B). Sph, spheroplasts; Peri, periplasm fraction. (C) Subcellular localization of the TapA protein**.** Cytoplasm/periplasm, inner membrane and outer membrane fractions of W83 (wild type), KDP385 (*ΔporT*::*erm*) and KDP383 (*ΔtapA*::*ermF*) were subjected to SDS-PAGE and immunoblot analysis using anti-TapA. Lanes: 1, cytoplasm/periplasm fraction; 2,

inner membrane fraction; 3, outer membrane fraction.

Fig. 6. Glycosylation of TapA protein.

TapA protein was immunoprecipitated from lysates of W83, KDP385 (*ΔporT*::*erm*) and KDP383 (*ΔtapA*::*ermF*) cells using anti-TapA. The resulting immunoprecipitates were subjected to SDS-PAGE and immunoblot analysis with MAb 1B5.

Fig. 7. Survival rates of mice challenged with the wild-type and mutant strains of *P. gingivalis*.

Construction of the *tapA, tapB, tapC* and *tapA tapB tapC* mutants is described in the Materials and Methods. Genetic manipulation did not affect the expression of downstream or upstream gene (Fig. S4 in the supplemental material). Female BALB/c mice were inoculated intradermally into the back with *P. gingivalis* cells (approximately 2 x 10^{11} CFU) and then their survival was monitored daily up to 9 days. The animal experiment in which five mice were used for each bacterial strain was performed three times. *P< 0.05 *versus* the corresponding values for the wild-type littermates, with the log-rank test.

Supplemental Material

Table S1. Oligonucleotides used in this study

Fig. S1. Real-time qPCR analysis of gene expression in the wild-type and *tprA* mutant strains.

Total RNA was isolated from *P. gingivalis* cells grown to mid-exponential phase ($OD_{600\ nm}$ of ~1.0) in enriched BHI broth. All PCR reactions were carried out in triplicate. Results are means ± SD (n=3).

Fig. S2. Transcriptional organization of the *tapA-tapB-tapC* locus.

To determine whether the *tapA-tapB-tapC* locus is transcribed in one polycistronic mRNA, we perfomed reverse transcriptional (RT) PCR. The intergenic spaces were amplified from a cDNA template. Lanes: 1, between PG2104 and PG2102 (*tapA*) (1,374 bp); 2, between PG2103 and PG2102 (*tapA*) (1,115 bp); 3, between PG2102 (*tapA*) and PG2101 (*tapB*) (1,150 bp); 4, between PG2101 (*tapB*) and PG2100 (*tapC*) (1,087 bp).

Fig. S3. No effect of *ermF* insertion on expression of the *tapB* gene downstream or upstream of the *ermF* insertion.

Whole cell lysates of *P. gingivalis* strains were subjected to SDS-PAGE and immunoblot analysis using anti-TapB. Lanes: 1, W83 (wild type); 2, KDP383 (*ΔtapA*::*ermF*); 3, KDP382 (*ΔtapB*::*ermF*); 4, KDP386 (*ΔtapC*::*ermF*).

Fig. S4. TPR proteins in *P. gingivalis* W83.

Locations of the TPR motif and signal peptide regions in TPR proteins are depicted. Square, TPR motif; Circle, His A kinase; Triangle, Histidine kinase-like ATPase. These

motifs were determined by Pfam 24.0 (http://pfam.sanger.ac.uk/). The signal peptide was determined by SignalP v3.0 and indicated by a thick line.

Table 1. Strains and plasmids used in this study

strain / plasmid	Description	source or ref.
P. gingivalis		
W83	wild type	
KDP159	*prA*::[*ermF ermAM*], Em^r	54
KDP382	*ΔtapB*::*ermF,* Em^r	this study
KDP383	*ΔtapA*::*ermF,* Em^r	this study
KDP384	*Δ*[*tapA tapB tapC*]::*ermF,* Em^r	this study
KDP385	*ΔporT*::[*ermF ermAM*], Em^r	this study
KDP386	*ΔtapC*::*ermF*, Em^r	this study
E. coli		
XL1-Blue	General-purpose host strain for cloning	stratagene
BL21(DE3)	host strain for expression vector pET-32a	Nippongene
S. cerevisiae		
AH109	host strain for yeast two-hybrid system	Clontech
plasmid		
pBluescript II SK(-)	Ap^r, cloning vector (pBSSK)	stratagene
pET-32a	Ap^r, expression vector	Novagen
pGEX-6P-1	Ap^r, expression vector	GE Healthcare
pKD357	Ap^r Em^r, pBSSK contains *ermF ermAM* cassette located between upstream and downstream of the *porT* gene	43
pKD1008	Ap^r, pBSSK contains 0.3-kb *tapC*-upstream and 0.5-kb *tapC*-downstream regions	this study
pKD1009	Ap^r Em^r, the *ermF* casassette was inserted into *Bam*HI site of pKD1008	this study
pKD1010	Ap^r, pBSSK contains 0.3-kb *tapB*-upstream and 0.5-kb *tapB*-downstream regions	this study
pKD1011	Ap^r Em^r, the *ermF* casassette was inserted into *Bam*HI site of pKD1010	this study
pKD1012	Ap^r, pBSSK contains 0.3-kb *tapA*-upstream and 0.5-kb *tapA*-downstream regions	this study
pKD1013	Ap^r Em^r, the *ermF* casassette was inserted into *Bam*HI site of pKD1012	this study
pKD1014	Ap^r, pBSSK contains 0.3-kb *tapA*-upstream and 0.5-kb *tapC*-downstream regions	this study
pKD1015	Ap^r Em^r, the *ermF* casassette was inserted into *Bam*HI site of pKD1014	this study
pKD1016	Ap^r, pET-32a containing *P. gingivalis tapB* gene	this study
pKD1017	Ap^r, pET-32a containing *P. gingivalis tapA* gene	this study
pKD1018	Ap^r, pGEX-6P-1 containing *P. gingivalis tprA* gene	this study
pKD1019	pGBKT7 containing *P. gingivalis tprA* gene	This study

Table 2. *P. gingivalis* genes differentially expressed in the *tprA* mutant cells placed in a mouse subcutaneous chamber compared to the wild-type cells

TIGR ID	Identification	Avr. fold difference
down-reglulated genes		
PG0100	hypothetical protein	0.59
PG0162	RNA polymerase sigma-70 factor, ECF subfamily	0.57
PG0591	ISPg5, transposase Orf2	0.63
PG0756	hypothetical protein	0.47
PG1055	thiol protease	0.36
PG1972	hemagglutinin protein HagB	0.63
PG1975	hemagglutinin protein HagC	0.64
PG2100 (*tapC*)	immunoreactive 63 kDa antigen PG102	0.34
PG2101 (*tapB*)	hypothetical protein	0.25
PG2102 (*tapA*)	immunoreactive 61 kDa antigen PG91	0.51
PG2103	hypothetical protein	0.24
PG2214	hypothetical protein	0.57
up-regulated genes		
PG0327	hypothetical protein	1.92
PG0373	hypothetical protein	1.72
PG0546	hypothetical protein	1.83
PG0635	ribosomal protein L11 methyltransferase	1.69
PG0656	ribosomal protein L34	2.02
PG0722	hypothetical protein	2.93
PG0969	S-adenosylmethionine:tRNA ribosyltransferase-isomerase, putative	1.98
PG1532	hypothetical protein	1.92
PG1866	hypothetical protein	1.93
PG2006	hypothetical protein	1.69
PG2225	hypothetical protein	1.63

Mouse subcutaneous chamber experiments were performed as described in "MATERIALS AND METHODS." Total RNA was extracted from W83 (wild type) and KDP159 (*tprA*::*erm*). Total RNA was extracted and analyzed by using a microarray as described in "MATERIALS AND METHODS." The number in the "Average fold difference" column indicates the gene expression in the *tprA* mutant versus the wild-type strain. The cut-off- ratio for the fold difference was 1.5.

Table 3. TprA-associated proteins predicted from yeast two-hybrid system

TIGR ID	description	Gene symbol	TIGR functional role category
putative periplasmic protein			
PG0415	peptidyl-prolyl cis-trans isomerase, PPIC-type		Protein fate: Protein folding and stabilization
PG0497	5'-methylthioadenosine/S-adenosylhomocysteine nucleosidase	*mtn*	Central intermediary metabolism: Other
PG1334	band 7/Mec-2 family protein		Unknown function: General
PG2101	hypothetical protein	*tapB*	
PG2200	TPR domain protein		Unknown function: General
putative inner membrane protein			
PG0081	hypothetical protein		
PG0093	HlyD family secretion protein		Transport and binding proteins: Other
PG0255	translation initiation factor IF-2	*infB*	Protein synthesis: Translation factors
PG0512	guanylate kinase	*gmk*	Purines, pyrimidines, nucleosides, and nucleotides: Nucleotide and nucleoside interconversions
PG1068	conserved hypothetical protein		Hypothetical proteins: Conserved
PG1271	acetylornithine aminotransferase, putative		Amino acid biosynthesis: Glutamate family
PG1490	TraG family protein		Mobile and extrachromosomal element functions: Plasmid functions
PG1768	magnesium chelatase, subunit D/I family		Transport and binding proteins: Cations and iron carrying compounds

PG1824	enolase	*eno*	Energy metabolism: Glycolysis/gluconeogenesis
PG2055	dihydroorotate dehydrogenase family protein		Purines, pyrimidines, nucleosides, and nucleotides: Pyrimidine ribonucleotide biosynthesis
PG1592	HDIG domain protein		Unknown function: General
PG1773	PAP2 superfamily protein		Unknown function: General

putative outer membrane protein

PG0026	hypothetical protein		
PG0421	hypothetical protein		
PG0809	hypothetical protein		

putative cytoplasmic protein

PG0065	efflux transporter, RND family, MFP subunit		Transport and binding proteins: Unknown substrate
PG0137	aminoacyl-histidine dipeptidase	*pepD-1*	Protein fate: Degradation of proteins, peptides, and glycopeptides
PG0153	aspartyl-tRNA synthetase	*aspS*	Protein synthesis: tRNA aminoacylation
PG0384	MutS2 family protein		DNA metabolism: Other
PG0394	DNA-directed RNA polymerase, beta subunit	*rpoB*	Transcription: DNA-dependent RNA polymerase
PG0395	DNA-directed RNA polymerase, beta' subunit	*rpoC*	Transcription: DNA-dependent RNA polymerase
PG0445	peptidase T	*pepT*	Protein fate: Degradation of proteins, peptides, and glycopeptides
PG0504	lipoate synthase	*lipA*	Biosynthesis of cofactors, prosthetic groups, and carriers: Lipoate
PG0520	chaperonin, 60 kDa	*groEL*	Protein fate: Protein folding and stabilization

PG0553	extracellular protease, putative		Protein fate: Degradation of proteins, peptides, and glycopeptides
PG0629	ATP-NAD kinase	*ppnK*	Biosynthesis of cofactors, prosthetic groups, and carriers: Pyridine nucleotides
PG0728	conserved hypothetical protein		Hypothetical proteins: Conserved
PG1195	8-amino-7-oxononanoate synthase	*bioF-2*	Biosynthesis of cofactors, prosthetic groups, and carriers: Biotin
PG1242	replicative DNA helicase	*dnaB*	DNA metabolism: DNA replication, recombination, and repair
PG1622	DNA topoisomerase IV, A subunit, putative		DNA metabolism: DNA replication, recombination, and repair
PG1849	DNA repair protein RecN	*recN*	DNA metabolism: DNA replication, recombination, and repair
PG1875	hemolysin		Cellular processes: Pathogenesis
PG1926	ribosomal protein L5	*rplE*	Protein synthesis: Ribosomal proteins: synthesis and modification
not detemined			
PG0232	zinc carboxypeptidase, putative		Protein fate: Degradation of proteins, peptides, and glycopeptides
PG1084	thioredoxin family protein		Energy metabolism: Electron transport

Fig. 1

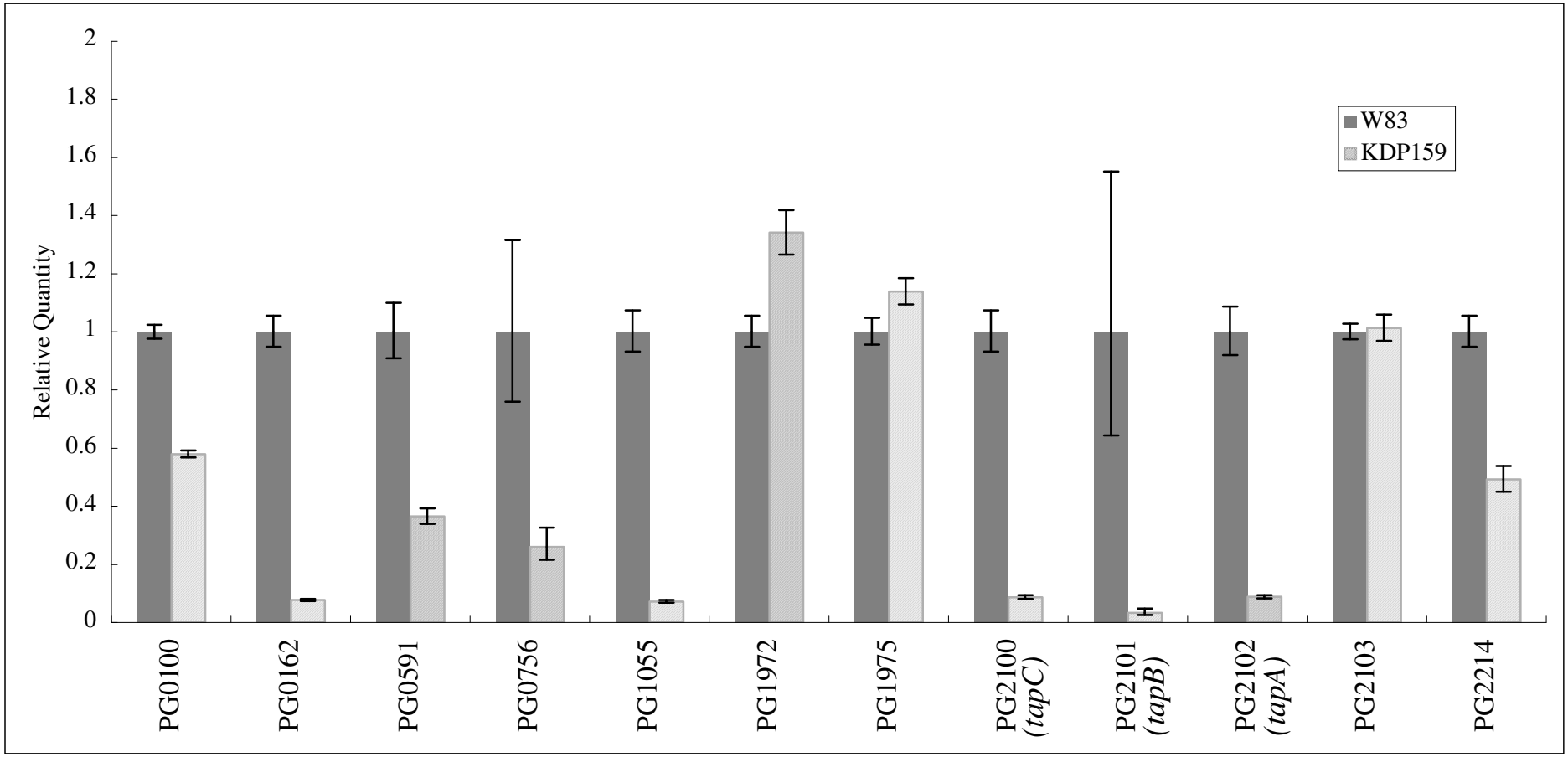
Relative Quantity
2
1.8
1.6
1.4
1.2
1
0.8
0.6
0.4
0.2
0
W83
KDP159
PG0100
PG0162
PG0591
PG0756
PG1055
PG1972
PG1975
PG2100 (tapC)
PG2101 (tapB)
PG2102 (tapA)
PG2103
PG2214

Fig. 2

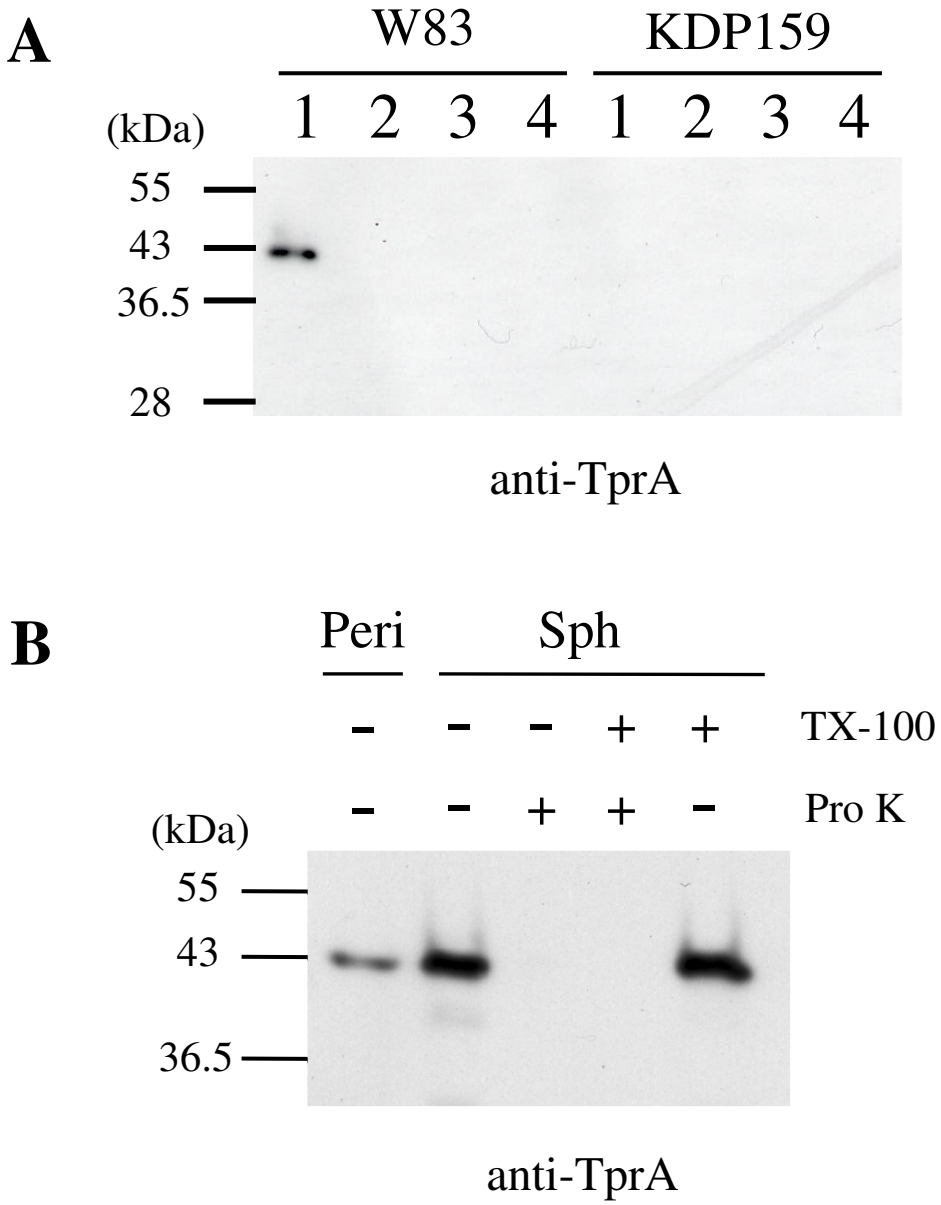
A
W83
KDP159
1 2 3 4 1 2 3 4
(kDa)
55
43
36.5
28
anti-TprA
B
Peri
Sph
- - - + + TX-100
- - + + - Pro K
(kDa)
55
43
36.5
anti-TprA

Fig. 3

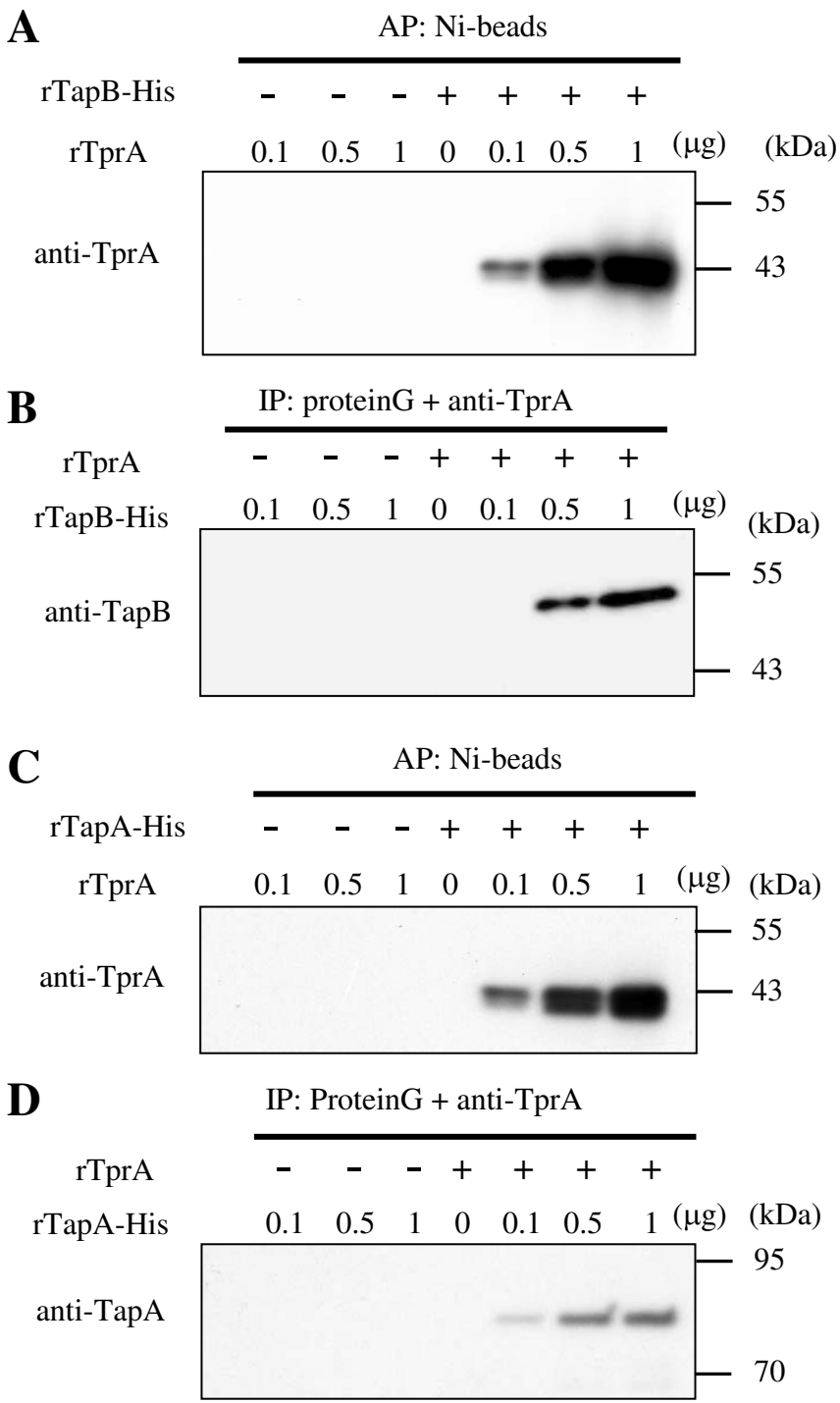
A
AP: Ni-beads
rTapB-His
- - - + + + +
rTprA
0.1 0.5 1 0 0.1 0.5 1 (μg)
(kDa)
anti-TprA
55
43
B
IP: proteinG + anti-TprA
rTprA
- - - + + + +
rTapB-His
0.1 0.5 1 0 0.1 0.5 1 (μg)
(kDa)
anti-TapB
55
43
C
AP: Ni-beads
rTapA-His
- - - + + + +
rTprA
0.1 0.5 1 0 0.1 0.5 1 (μg)
(kDa)
anti-TprA
55
43
D
IP: ProteinG + anti-TprA
rTprA
- - - + + + +
rTapA-His
0.1 0.5 1 0 0.1 0.5 1 (μg)
(kDa)
anti-TapA
95
70

Fig. 4

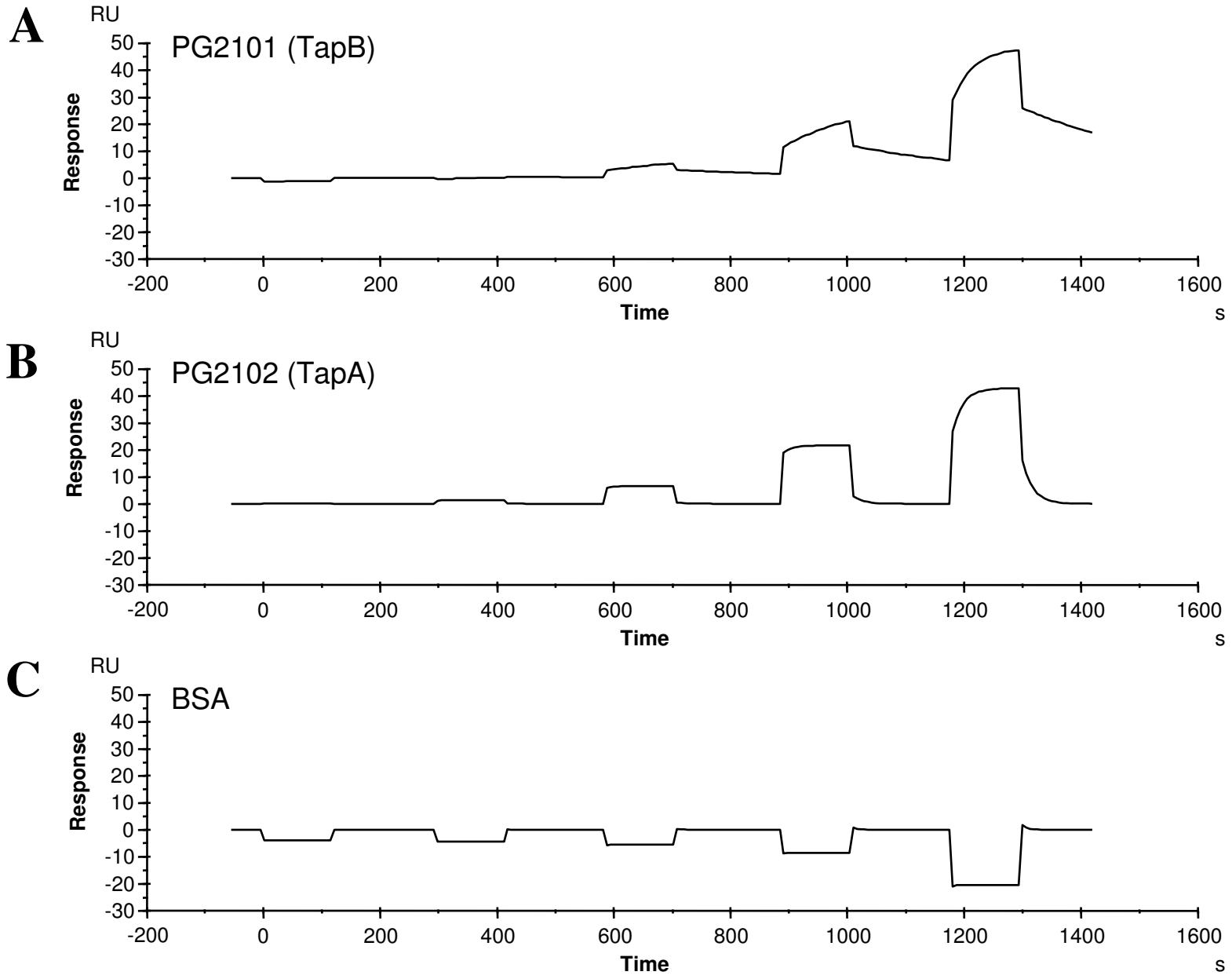
A
RU
PG2101 (TapB)
Response
50
40
30
20
10
0
-10
-20
-30
-200
0
200
400
600
800
1000
1200
1400
1600
Time
s
B
RU
PG2102 (TapA)
Response
Time
s
C
RU
BSA
Response
Time
s

Fig. 5

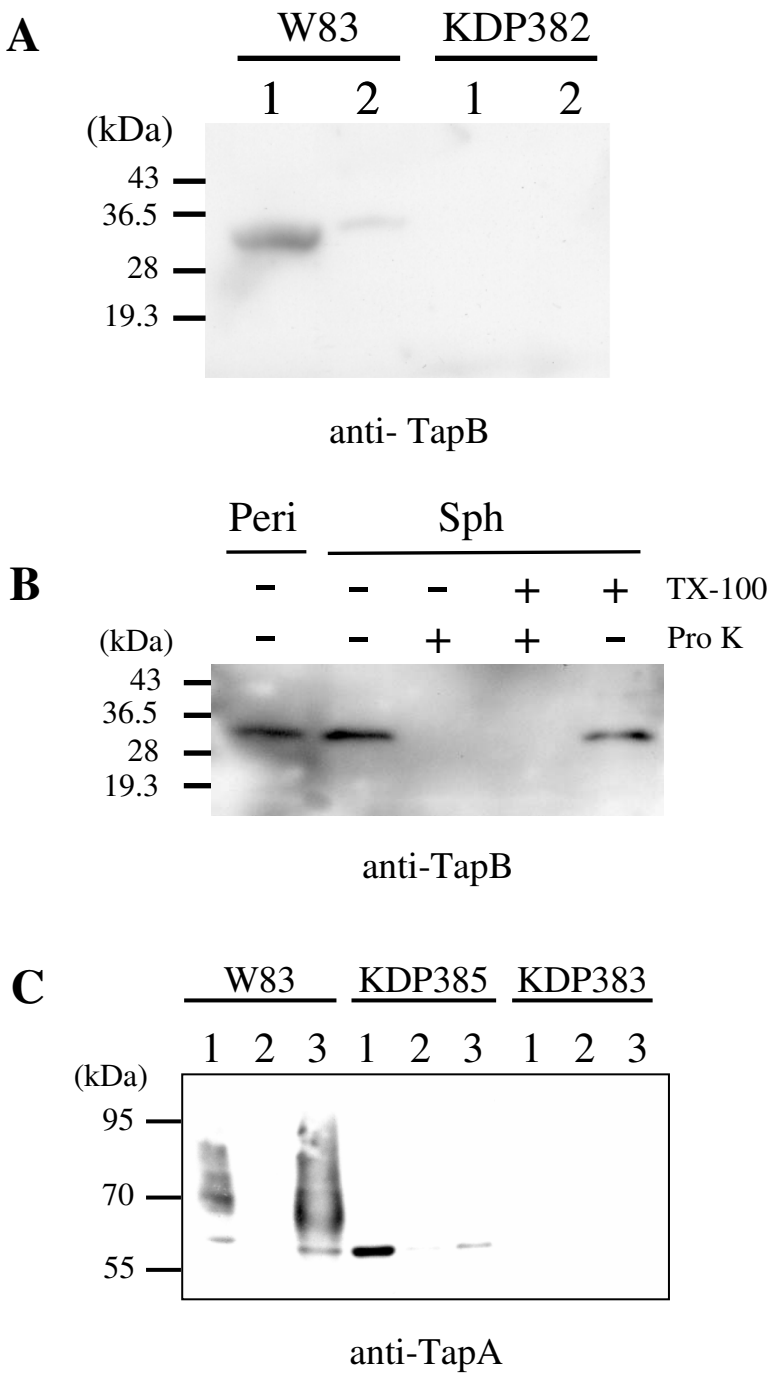
A
W83
KDP382
1
2
1
2
(kDa)
43
36.5
28
19.3
anti- TapB
B
Peri
Sph
- - - + + TX-100
(kDa) - - + + - Pro K
43
36.5
28
19.3
anti-TapB
C
W83
KDP385
KDP383
1 2 3 1 2 3 1 2 3
(kDa)
95
70
55
anti-TapA

Fig. 6

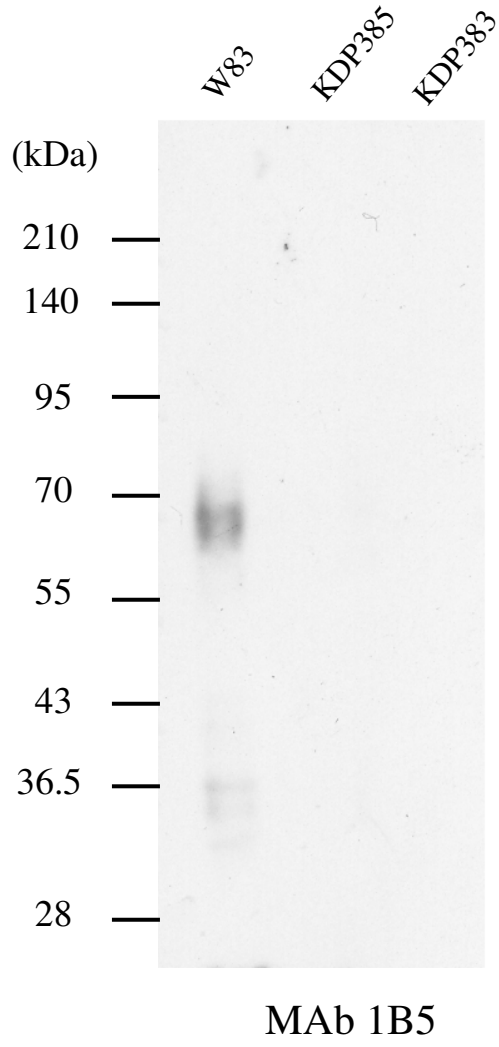

Fig. 7

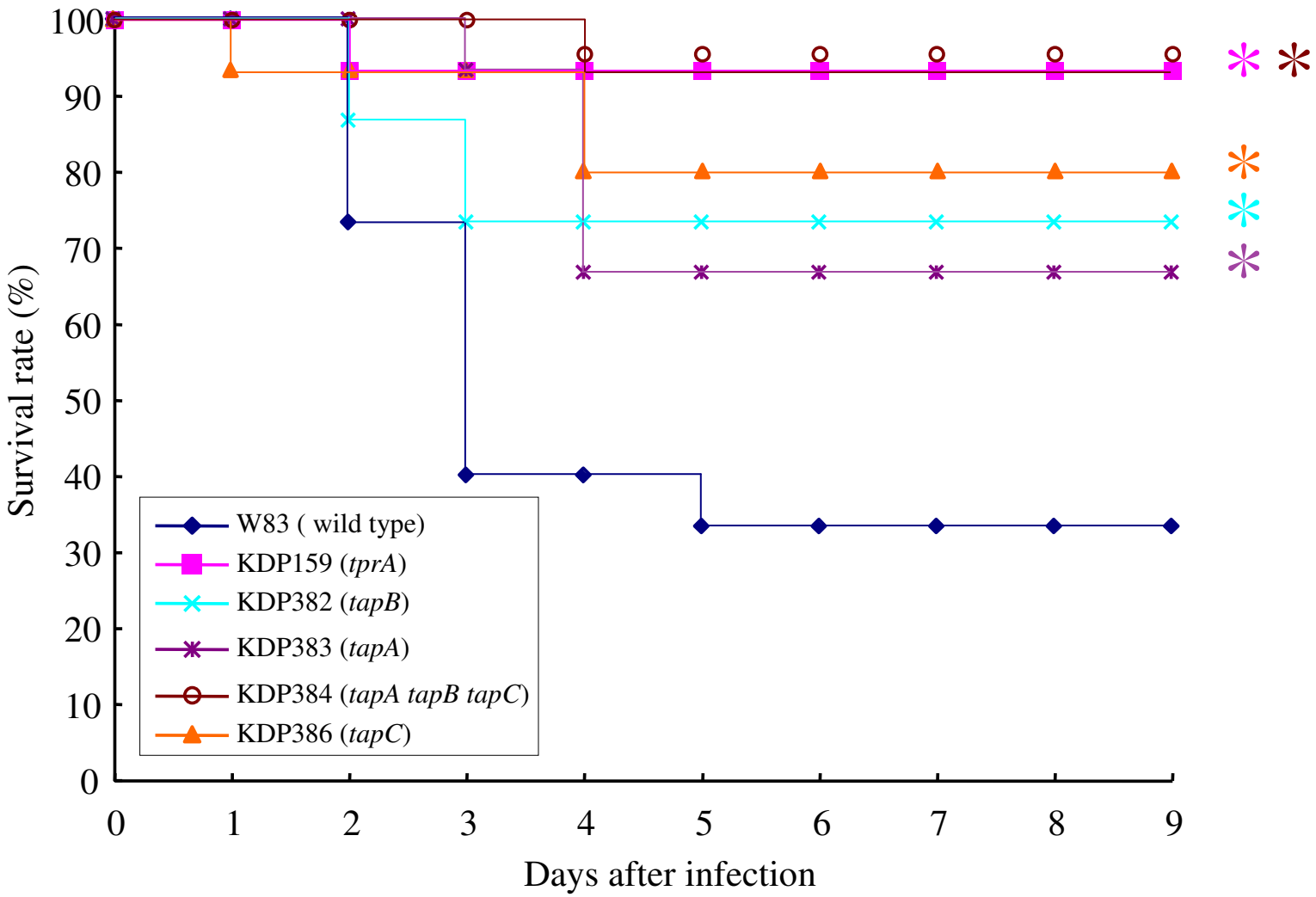
Survival rate (%)
100
90
80
70
60
50
40
30
20
10
0
0
1
2
3
4
5
6
7
8
9
Days after infection
W83 (wild type)
KDP159 (tprA)
KDP382 (tapB)
KDP383 (tapA)
KDP384 (tapA tapB tapC)
KDP386 (tapC)
*
*
*
*
*

Table S1. Oligonucleotides used in this study

Oligonucleotide	Sequence (5'-3')
construction of mutant strains	
5-PG2100up/NotI	gcggccgcatgccaagaattatgaaattaa
3-PG2100up/BamHI	ggatccgcaatgcgagacatcgaagtcata
5-PG2100dn/BamHI	ggatccgagatacagatggatcaaatacga
3-PG2100dn/KpnI	ggtaccttactctacaatgatttttccac
5-PG2100up/NotI	gcggccgcttgtctctaaaaagcaacgcta
3-PG2100up/BamHI	ggatccttccagttcttgcagagagatcgt
5-PG2100dn/BamHI	ggatccacggccaaaggaatgaaaataacc
3-PG2100dn/KpnI	ggtaccctactccagcttcgtgagcagcgt
5-PG2100up/NotI	gcggccgcatgaagacaaaagttttacgca
3-PG2100up/BamHI	ggatccgaagtcttgaaactgataatcatc
5-PG2100dn/BamHI	ggatcccaagaacgccaatcactacctgat
3-PG2100dn/KpnI	ggtaccttattccacgatgagcttctctac
real-time qPCR	
realPG0347-Fw	tgctgtgctcgacggtatag
realPG0347-Rv	attcgcctacggccttactt
realPG1386-Fw	tcattggggaatttgtggat
realPG1386-Rv	gtctttggaggaacggatga
realPG0100-Fw	ttgtactacacttttgttcttcgtatg
realPG0100-Rv	aaagagccgattgattttgc
realPG0162-Fw	tgtcccggtatgatgctgta
realPG0162-Rv	gactgcaatctggctccttc
realPG0591-Fw	gagctcatggtgctttgtca
realPG0591-Rv	acaaggagttccccaggtct
realPG0756-Fw	ggcgaagatgggactgaata
realPG0756-Rv	tgcggacgaatcacatacat
realPG1055-Fw	acctcctcgggaaaactcat
realPG1055-Rv	ctcagtcactccccatggat
realPG1972-Fw	tttgccaagaatgtgctgac
realPG1972-Rv	gtcgagggctatgacctgag
realPG1975-Fw	tttgccaagaatgtgctgac

realPG1975-Rv	gtcgagggctatgacctgag
realPG2100-Fw	gcgtggtctgaaccgataat
realPG2100-Rv	tatacgtaatggcccgggta
realPG2101-Fw	ccgattactctgcgaaccat
realPG2101-Rv	gcttgcccttcttgtcgtag
realPG2102-Fw	gctttggctttcgcttacac
realPG2102-Rv	tggattcagaggtgctaccc
realPG2103-Fw	gcgcgatttgtccaagtatatc
realPG2103-Rv	aaaatcgaaatcggcaattc
realPG2214-Fw	gtcgagggctatgacctgag
realPG2214-Rv	gccagttctttagcggacac
reverse transcriptional PCR	
RT-2104-Fw	atgcgcaagacatctctttgtttttcttt
RT-2103-Fw	atgcgtgatttgtccaagaaaatgcgcgat
RT-2102-Rv	ttgtcgacaaagttcgacaagaaaccgata
RT-2102-Fw	atttacgtatacatcatctgccaatgctct
RT-2101-Rv	attcctttggccgtattcgttacgctctgt
RT-2101-Fw	tggtgcgacggcgaccgattctatgtcgat
RT-2100-Rv	cgatggctacacccatcagtctattattag
preparation for recombinant proteins	
5-rPG1385/BamHI	ggatccatgaacaagaaaagtttattggca
3-rPG1385/EcoRI	gaattcttttccttcgtgacgctctgtcag
5-rPG2100/KpnI	ggtaccatggatattggtggagacgatgta
3-rPG2100/NotI	gcggccgcctctacaatgatttttccacg
5-rPG2101/KpnI	ggtaccatgcagggatattgtatgccccaa
3-rPG2101/NotI	gcggccgcctccagcttcgtgagcagcgta
5-rPG2102/KpnI	ggtaccatgggaggagatgatgtcaaggtg
3-rPG2102/NotI	gcggccgcttccacgatgagcttctctacg
yeast two-hybrid system	
Y2H-PG1385-Fw	ccatggatgaacaagaaaagtttattggca
Y2H-PG1385-Rv	ggatccttttccttcgtgacgctctgtcag

Figure S1

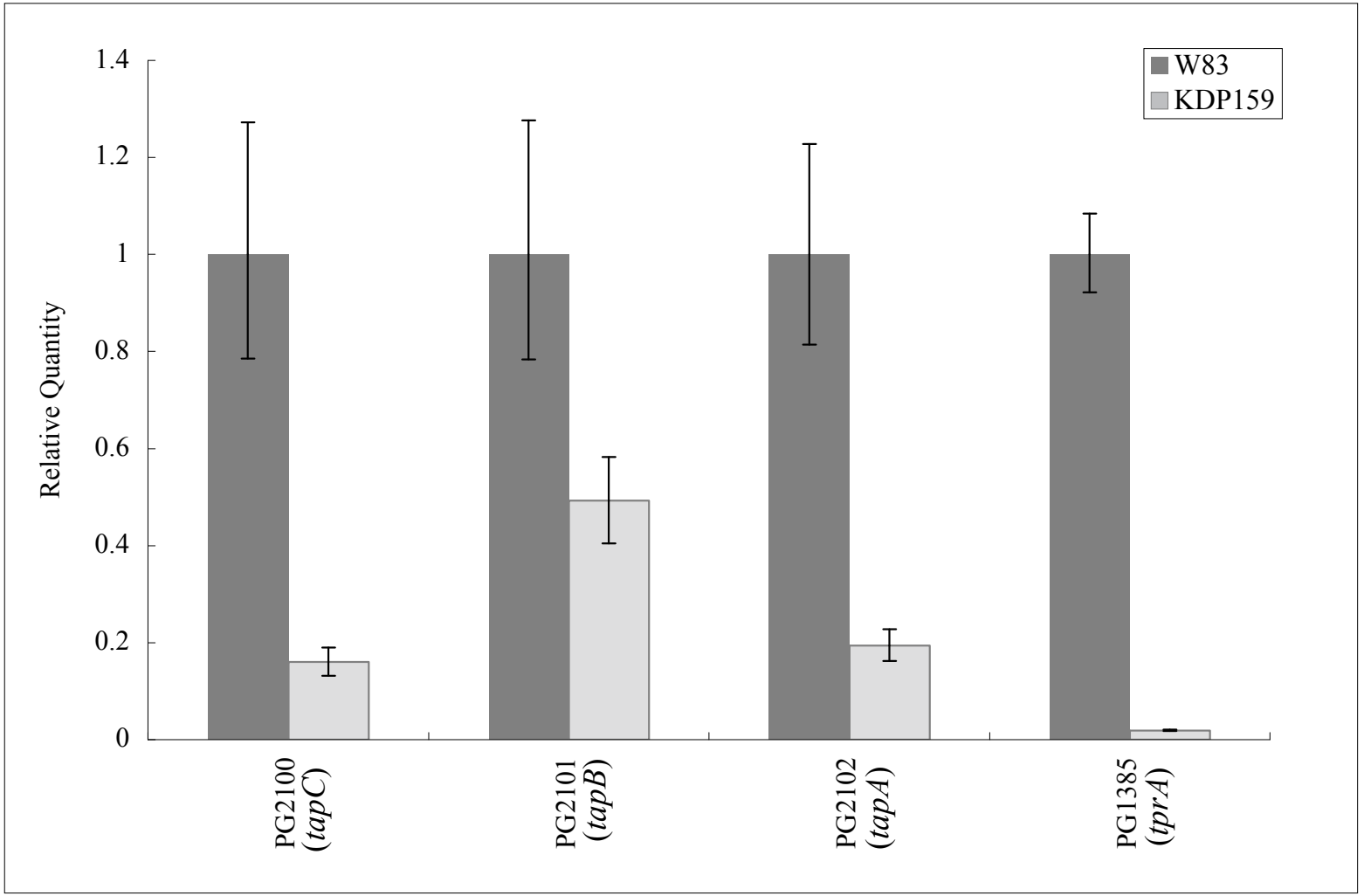
W83
KDP159
Relative Quantity
1.4
1.2
1
0.8
0.6
0.4
0.2
0
PG2100 (tapC)
PG2101 (tapB)
PG2102 (tapA)
PG1385 (tprA)

Figure S2

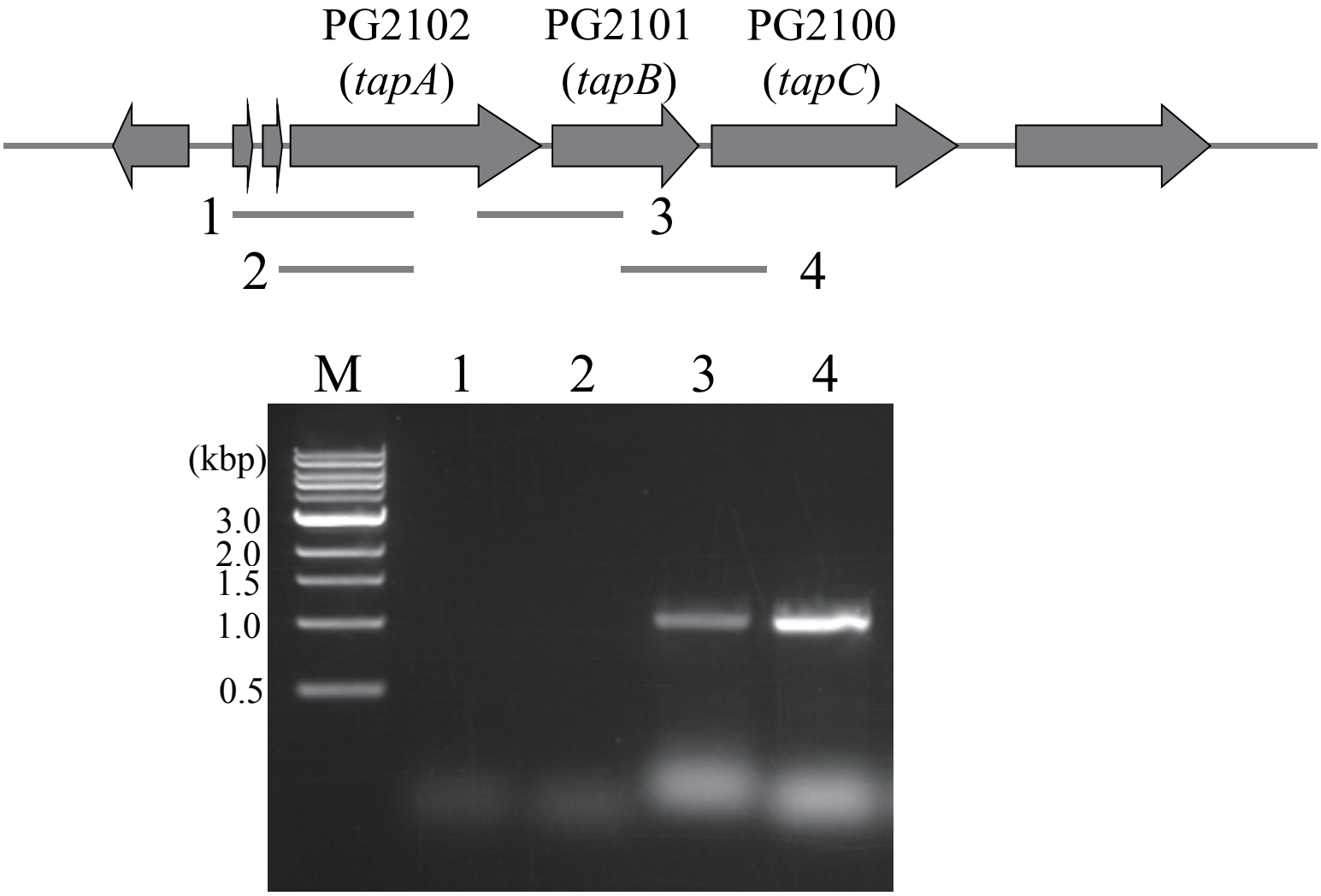
PG2102
(tapA)
PG2101
(tapB)
PG2100
(tapC)
1
2
3
4
M
1
2
3
4
(kbp)
3.0
2.0
1.5
1.0
0.5

Figure S3

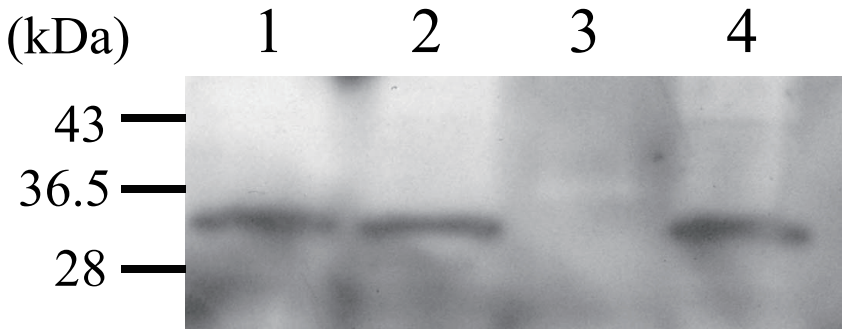

Figure S4

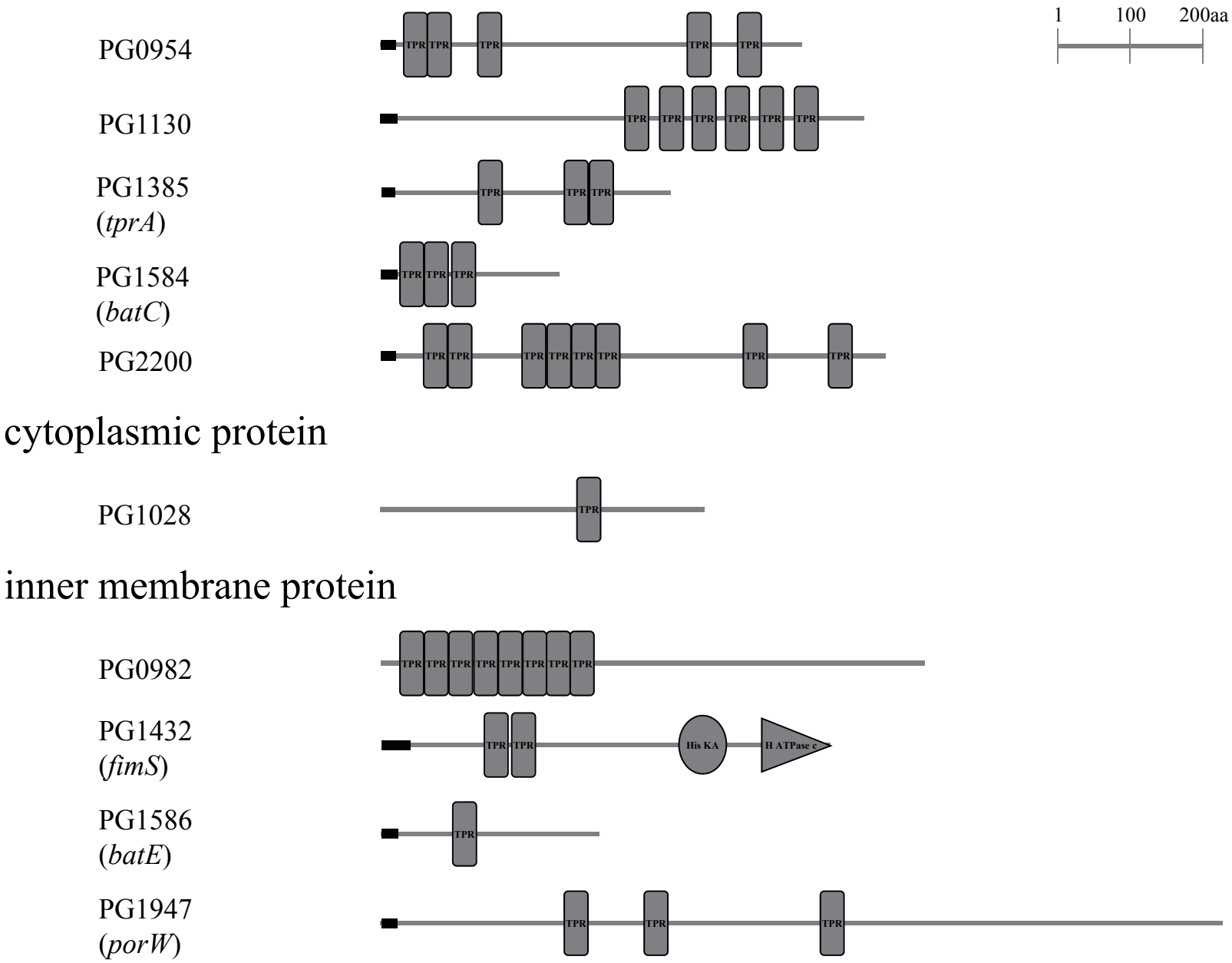
periplasmic protein
PG0954
PG1130
PG1385
(tprA)
PG1584
(batC)
PG2200
1
100
200aa
TPR
cytoplasmic protein
PG1028
inner membrane protein
PG0982
PG1432
(fimS)
PG1586
(batE)
PG1947
(porW)
His KA
H ATPase c